SUPPLEMENTAL DATA

An adipocyte-endothelial framework linking adipose tissue inflammation to cardiometabolic vulnerability in obesity

Vaishali Chaurasiya[1,2,#], Luyang Li[3,4,#], Aina Lluch[5,6,#], Ana Fernández-Sánchez[5], Jukka Harju[7], Dan Duc Pham[1], Sanni Perttunen[1], Salla Keskitalo[8], Markku Varjosalo[8], Kirsi H. Pietiläinen[9,10], P.A. Nidhina Haridas[1], José M. Moreno-Navarrete[5,6,11], José I. Rodríguez-Hermosa[5,11], Encarna Piedrafita-Serra[5,11], Asha Kar[12,13], Päivi Pajukanta[12,13], Markku Laakso[14], Ville Männistö[14], Jussi Pihlajamäki[15], Minna U. Kaikkonen[16], Gema Frühbeck[6,17], Oriol A. Rangel-Zúñiga[6,18], Francisco J. Tinahones[6,19], Carlos Diéguez[6,20], Ralph Burkhardt[21], Marcus Höring[21], Gerhard Liebisch[21], Johanna Pörschke[22], María Gómez-Serrano[22], Johannes Graumann[23], Witold Szymanski[23], José M. Fernández-Real[5,6,11], You Zhou[3,4], Vesa M. Olkkonen[1,24,*], Francisco J. Ortega[5,6,**]

[1] Minerva Foundation Institute for Medical Research, Biomedicum 2U – Helsinki, Finland
[2] Doctoral Programme in Clinical Research, University of Helsinki – Helsinki, Finland
[3] Division of Infection and Immunity, School of Medicine, Cardiff University – Cardiff, United Kingdom
[4] Systems Immunity Research Institute, Cardiff University – Cardiff, United Kingdom
[5] Girona Biomedical Research Institute – Girona, Spain
[6] CIBER de la Fisiología de la Obesidad y la Nutrición – Madrid, Spain
[7] Department of Gastrointestinal Surgery, Abdominal Center, University of Helsinki and Helsinki University Hospital – Helsinki, Finland
[8] Molecular Systems Biology Research Group & Proteomics Unit, HiLIFE Helsinki Institute of Life Science, Institute of Biotechnology, University of Helsinki – Helsinki, Finland
[9] Obesity Research Unit, Research Program for Clinical and Molecular Metabolism, Faculty of Medicine, Helsinki University Hospital, University of Helsinki – Helsinki, Finland
[10] HealthyWeightHub, Endocrinology, Abdominal Center, Helsinki University Hospital – Helsinki, Finland
[11] School of Medicine, University of Girona – Girona, Spain
[12] Bioinformatics Interdepartmental Program, UCLA – Los Angeles, USA
[13] Institute for Precision Health, David Geffen School of Medicine at UCLA – Los Angeles, USA
[14] Institute of Clinical Medicine, University of Eastern Finland and Kuopio University Hospital – Kuopio, Finland
[15] Institute of Public Health and Clinical Nutrition, University of Eastern Finland and Kuopio University Hospital – Kuopio, Finland
[16] A.I. Virtanen Institute for Molecular Sciences, University of Eastern Finland – Kuopio, Finland
[17] Instituto de Investigación Sanitaria de Navarra (IdISNA), Clínica Universidad de Navarra – Pamplona, Spain
[18] Maimónides Biomedical Research Institute of Córdoba (IMIBIC), Reina Sofia University Hospital, University of Córdoba – Córdoba, Spain
[19] Instituto de Investigación Biomédica de Málaga (IBIMA), Virgen de la Victoria Hospital, University of Málaga – Málaga, Spain
[20] Center for Research in Molecular Medicine and Chronic Diseases (CiMUS, University of Santiago de Compostela, Instituto de Investigación Sanitaria – Santiago de Compostela, Spain
[21] Institute of Clinical Chemistry and Laboratory Medicine, University Hospital Regensburg – Regensburg, Germany
[22] Institute for Tumor Immunology, Center for Tumor Biology and Immunology, Marburg University – Marburg, Germany
[23] Institute of Translational Proteomics & Core Facility, Marburg University – Marburg, Germany
[24] Department of Anatomy, Faculty of Medicine, University of Helsinki – Helsinki, Finland
[#] Equal contribution

Corresponding authors:
*V. M. Olkkonen, Ph.D. email: vesa.olkkonen@helsinki.fi
**F. J. Ortega, Ph.D. email: fortega@idibgi.org

Short title: Signatures of meta-inflammation in adipose tissue.

SUPPLEMENTARY TABLES

Supplementary Table S1. Clinical and biochemical data of cholecystectomy patients (cohort #1) in which omental adipose tissue was collected for adipocyte and endothelial cell isolation.

Cross-sectional study			
Parameters	Lean (n=9)	Obese (n=8)	p-value[a]
Age (years)	48 ± 11.5	45 ± 9.8	0.499
Sex (men/women)	0/8	2/7	n/a
BMI (kg/m^2)	23.1 ± 1.6	34.1 ± 2.6	<0.0001
Glucose (mg/dl)	92.7 ± 6.1	100.7 ± 7.4	0.030
HbA1c (%)	5 ± 0.2	5.4 ± 0.3	0.011
Insulin (mIU/l)	4.6 ± 1.7	19.4 ± 12.6	0.007
HOMA-IR	1.1 ± 0.4	4.8 ± 3.5	0.009
Cholesterol (mg/dl)	168.5± 21.5	176 ± 22.5	0.484
LDL (mg/dl)	106.8 ± 25.2	133.5 ± 30.4	0.058
HDL (mg/dl)	55.3 ± 11.4	41.2 ± 9.3	0.016
Triglycerides (mg/dl)	88.6 ± 39.5	123.9 ± 35.9	0.101

Values show the mean ± S.D. BMI: body mass index; HbA1C: glycated hemoglobin; HOMA-IR: homeostatic model assessment for insulin resistance (where > 2 indicate insulin resistance); H/LDL: high/low-density lipoproteins. [a] Results obese vs lean were compared by unequal variance *t*-test. n/a, no applies.

Supplementary Table S2. Anthropometric and biochemical data depicting cohort #2, including 18 gastric bypass patients with severe obesity before (baseline) and after weight loss (post-WL).

Longitudinal study			
Parameters	Baseline	Post-WL	p-value[a]
Age (years)	48 ± 10	51 ± 10	<0.0001
Sex (men/women)	2/16		n/a
BMI (kg/m^2)	42.8 ± 4.9	28.6 ± 5.5	<0.0001
SBP (mmg)	128.2 ± 14.6	129.6 ± 16.0	0.721
DBP (mmg)	80.4 ± 10.2	74.4 ± 14.2	0.136
Glucose (mg/dl)	102.7 ± 41.0	88.4 ± 15.7	0.178
HbA1c (%)	6.0 ± 1.6	5.3 ± 0.4	0.112
Cholesterol (mg/dl)	180.9 ± 54.0	174.9 ± 30.3	0.607
LDL (mg/dl)	99.2 ± 26.3	96.8 ± 25.2	0.708
HDL (mg/dl)	54.7 ± 14.1	74.9 ± 24.1	<0.0001
Triglycerides (mg/dl)	105.2 ± 36.5	86.7 ± 31.0	0.072

Values show the mean ± S.D. BMI: body mass index; S/DBP: systolic/diastolic blood pressure; HbA1C: glycated hemoglobin; H/LDL: high/low-density lipoproteins. [a] Results post-weight loss *vs* baseline were compared by paired *t*-test. n/a, no applies.

Supplementary Table S3. Clinical and biochemical parameters of subjects included in the cross-sectional study METSIM (cohort #3).

N	335
Sex (% men)	100
Age (years)	54 ± 5
BMI (kg/m^2)	26.8 ± 3.7
SBP (mmHg)	133.9 ± 14.7
DBP (mmHg)	87.4 ± 9
Fasting glucose (mg/dl)	103.3 ± 8.9
HbA1c (%)	5.6 ± 0.3
Total cholesterol (mg/dl)	212.4 ± 33.3
LDL cholesterol (mg/dl)	135.6 ± 28.4
HDL cholesterol (mg/dl)	56.7 ± 14
Fasting triglycerides (mg/dl)	121.5 ± 73.1

Data are expressed as mean ± S.D. BMI: body mass index; S/DBP: systolic/diastolic blood pressure; HbA1c: glycated hemoglobin; H/LDL: high/low-density lipoproteins.

Supplementary Table S4. Clinical and biochemical parameters of subjects included in our cross-sectional study from the ADIPOMIT cohort (cohort #5). Only participants with BMI≥30 kg/m^2 were included.

Parameters	All	HO	UO	p-value[a]
N	451	83	368	n/a
Sex (% men)	30.6	36.1	29.9	n/a
Age (years)	46 ± 10	45 ± 9	47 ± 10	0.24
BMI (kg/m^2)	46.8 ± 7.9	43.5 ± 8.2	47.4 ± 7.3	<0.0001
SBP (mmHg)	135.9 ± 18.8	136.7 ± 17.0	135.9 ± 19.1	0.744
DBP (mmHg)	81.7 ± 12.8	80.0 ± 12.1	82.3 ± 12.8	0.151
Fasting glucose (mg/dl)	109.0 ± 31.2	88.1 ± 7.9	113.8 ± 32.5	<0.0001
HbA1c (%)	6.1 ± 1.3	5.4 ± 0.6	6.3 ± 1.4	<0.0001
Total cholesterol (mg/dl)	178.8 ± 41.3	184.9 ± 33.9	177.6 ± 42.8	0.149
HDL cholesterol (mg/dl)	108.0 ± 32.9	61.2 ± 20.5	42.4 ± 15.1	<0.0001
LDL cholesterol (mg/dl)	45.8 ± 17.7	111.1 ± 27.2	107.4 ± 34.0	0.354
Fasting triglycerides (mg/dl)	138.6 ± 71.0	96.2 ± 28.0	148.0 ± 74.3	<0.0001

Data are expressed as mean ± S.D. BMI: body mass index; S/DBP: systolic/diastolic blood pressure; HbA1c: glycated hemoglobin; H/LDL: high/low-density lipoproteins. [a] Results metabolically "unhealthy" (UO) *vs* "healthy" (HO) obesity were compared by Student *t*-test. n/a, no applies.

Supplementary Table S5. Clinical and biochemical parameters of subjects included in the KOBS cohort (cohort #6). Only participants with BMI≥30 kg/m^2 were included.

Parameters	All	HO	UO	p-value[a]
N	241	22	219	n/a
Sex (% men)	30.7	40.9	29.7	n/a
Age (years)	48.8 ± 9.1	49.1 ± 9.2	48.8 ± 9.2	0.867
BMI (kg/m^2)	43.1 ± 5.3	40.9 ± 3.6	43.3 ± 5.4	0.008
Fasting glucose (mg/dl)	118 ± 35.8	93.2 ± 5.4	120.5 ± 36.6	<0.0001
Total cholesterol (mg/dl)	159.5 ± 34.9	159.1 ± 24.4	159.6 ± 35.9	0.932
HDL cholesterol (mg/dl)	42.9 ± 11.4	56.9 ± 11.2	41.5 ± 10.5	<0.0001
LDL cholesterol (mg/dl)	89.3 ± 31.1	84.7 ± 21.8	89.8 ± 31.9	0.327
Fasting triglycerides (mg/dl)	137.9 ± 61.4	88.6 ± 23.3	142.9 ± 61.9	<0.0001

Data are expressed as mean ± S.D. BMI: body mass index; H/LDL: high/low-density lipoproteins. [a] Results metabolically "unhealthy" (UO) *vs* "healthy" (HO) obesity were compared by Student *t*-test. n/a, no applies.

Supplementary Table S6. Proteomics specifics.

Study	Sample	Sample preparation	Liquid chromatography	MS Instrument
#1a	Bulk adipose tissue	SP3-C18	nanoElute 2	Bruker TimsTof Ultra
#2a	Isolated adipocytes	Methanol/chloroform-C18	Evosep One	Bruker TimsTof Pro 2
#2b	Isolated EC	Methanol/chloroform-C18	Evosep One	Bruker TimsTof Pro 2
#3a	In vitro adipogenesis	SP3-C18	nanoElute 2	Bruker TimsTof Pro
#3b	MCM-adipocytes	SP3-C18	nanoElute 2	Bruker TimsTof Pro
#3c	MCM-HAMEC	SP3-C18	nanoElute 2	Bruker TimsTof Ultra
#3d	ACM-HAMEC	Methanol/chloroform-C18	Evosep One	Bruker TimsTof Pro 2

Study	Analytical column	MS method	LC method	Spectrum matching
#1a	Bruker PepSep Ultra	DIA-PASEF_sens_0.96s.m	30min_psULTRA_oneCol	Dia-NN
#2a	Evosep EV1109-60/100 SPD	DDA-PASEF-short_gradient_0.5s.m	Evosep_60SPD_21min	FragPipe
#2b	Evosep EV1109-60/100 SPD	DDA-PASEF-short_gradient_0.5s.m	Evosep_60SPD_21min	FragPipe
#3a	IonOptics Aurora Ultimate™	DIA-PASEF_long gradient.m	Bruker_default_100min_gradient	Dia-NN
#3b	IonOptics Aurora Ultimate™	DIA-PASEF_long gradient.m	Bruker_default_100min_gradient	Dia-NN
#3c	Bruker PepSep Ultra	DIA-PASEF_norm_0.96s.m	45min_psULTRA_twoCol	Dia-NN
#3d	Evosep EV1137-30 SPD	DIA-PASEF-short_gradient.m (DIA windows)	Evosep_30SPD_44min	Dia-NN

Study	Database	Autonomics	Computed values for statistics
#1a	UniProt_Human_canonical_012024_20429entries.fasta	1.15.145	Log_2 intensity
#2a	2023-12-18_decoys_reviewed_contam_UP000005640.fas	1.17.16	Log_2 intensity
#2b	2023-12-18_decoys_reviewed_contam_UP000005640.fas	1.17.16	Log_2 intensity
#3a	UniProt_Human_canonical_042023_20407entries.fasta	1.1.7.14	Max LFQ
#3b	UniProt_Human_canonical_042023_20407entries.fasta	1.1.7.14	Max LFQ
#3c	UniProt_Human_canonical_112024_20429entries.fasta	1.15.235	Max LFQ
#3d	UniProtKB_Taxonomy_ID_9606_AND_reviewed_2025_02_06.fasta	1.15.345	Max LFQ

Supplementary Table S7. Functional enrichment of proteins significantly modulated in "obese" vs "lean" isolated adipocytes. Only top 10 terms included in the classification Biological Processes (BP) and Cellular Components (CC) as noted in the Gene Ontology (GO) database are listened below. Abundance changes affecting proteins annotated in categories of interest are represented in **Figure 1c**. For additional details, see in the **Source Data file**, with source data underlying the plots contained in this article.

#	source	term_name	term_id	Adj._p-value	term_size	intersection_size
1	GO:BP	cellular respiration	GO:0045333	8.01E-61	73	245
2	GO:BP	energy derivation by oxidation of organic compounds	GO:0015980	1.16E-59	82	352
3	GO:BP	aerobic respiration	GO:0009060	1.18E-59	67	201
4	GO:BP	generation of precursor metabolites and energy	GO:0006091	2.66E-58	91	484
5	GO:BP	oxidative phosphorylation	GO:0006119	9.60E-44	50	151
6	GO:BP	organic acid catabolic process	GO:0016054	2.66E-42	58	242
7	GO:BP	carboxylic acid catabolic process	GO:0046395	2.66E-42	58	242
8	GO:BP	cellular catabolic process	GO:0044248	1.63E-41	64	323
9	GO:BP	small molecule catabolic process	GO:0044282	6.57E-40	66	370
10	GO:BP	nucleoside phosphate biosynthetic process	GO:1901293	4.14E-36	59	322
1	GO:CC	oxidoreductase complex	GO:1990204	2.13E-50	54	153
2	GO:CC	respiratory chain complex	GO:0098803	4.95E-44	44	109
3	GO:CC	tricarboxylic acid cycle heteromeric enzyme complex	GO:0045239	2.47E-15	12	17
4	GO:CC	nucleoid	GO:0009295	2.47E-15	17	49
5	GO:CC	mitochondrial nucleoid	GO:0042645	2.47E-15	17	49
6	GO:CC	alpha-ketoacid dehydrogenase complex	GO:0045240	9.70E-15	12	19
7	GO:CC	Nadh dehydrogenase complex	GO:0030964	1.28E-14	16	46
8	GO:CC	respiratory chain complex i	GO:0045271	1.28E-14	16	46
9	GO:CC	proton-transporting atp synthase complex	GO:0045259	8.37E-14	11	17
10	GO:CC	mitochondrial protein-containing complex	GO:0098798	6.81E-13	25	178

Supplementary Table S8. Functional enrichment of proteins significantly modulated during adipogenesis. Only top 10 terms included in the classification Biological Processes (BP) and Cellular Components (CC) as noted in the Gene Ontology (GO) database are listened below. Abundance changes affecting proteins annotated in categories of interest are represented in **Figure S5c**. For additional details, see in the **Source Data file**, with source data underlying the plots contained in this article.

#	source	term_name	term_id	adj._p-value	term_size	intersection_size
1	GO:BP	small molecule catabolic process	GO:0044282	2.97E-17	91	375
2	GO:BP	fatty acid metabolic process	GO:0006631	1.05E-16	93	401
3	GO:BP	organic acid catabolic process	GO:0016054	1.05E-16	70	252
4	GO:BP	carboxylic acid catabolic process	GO:0046395	1.05E-16	70	252
5	GO:BP	fatty acid beta-oxidation	GO:0006635	3.22E-15	35	76
6	GO:BP	purine nucleotide metabolic process	GO:0006163	4.03E-14	96	463
7	GO:BP	purine-containing compound metabolic process	GO:0072521	1.04E-13	99	493
8	GO:BP	fatty acid catabolic process	GO:0009062	1.90E-12	38	106
9	GO:BP	lipid oxidation	GO:0034440	4.39E-12	39	114
10	GO:BP	monocarboxylic acid catabolic process	GO:0072329	4.87E-12	42	131
1	GO:CC	collagen-containing extracellular matrix	GO:0062023	1.49E-18	98	429
2	GO:CC	mitochondrial matrix	GO:0005759	1.49E-18	106	487
3	GO:CC	focal adhesion	GO:0005925	2.52E-18	96	421
4	GO:CC	cell-substrate junction	GO:0030055	3.17E-18	97	431
5	GO:CC	organelle outer membrane	GO:0031968	6.04E-11	57	246
6	GO:CC	outer membrane	GO:0019867	7.22E-11	57	248
7	GO:CC	mitochondrial outer membrane	GO:0005741	1.16E-10	52	217
8	GO:CC	oxidoreductase complex	GO:1990204	5.20E-10	37	128
9	GO:CC	peroxisome	GO:0005777	8.19E-10	39	143
10	GO:CC	microbody	GO:0042579	8.19E-10	39	143

Supplementary Table S9. Functional enrichment of proteins significantly modulated in MCM-activated adipocytes. Only top 10 terms are listened below. Abundance changes affecting proteins annotated in categories of interest are represented in **Figure 3c**. For further details, see in the **Source Data file**.

#	source	term_name	term_id	adj._p-value	term_size	intersection_size
1	GO:BP	cellular respiration	GO:0045333	1.37E-55	83	243
2	GO:BP	energy derivation by oxidation of organic compounds	GO:0015980	1.97E-49	89	337
3	GO:BP	aerobic respiration	GO:0009060	3.87E-48	70	197
4	GO:BP	organic acid catabolic process	GO:0016054	2.60E-42	72	252
5	GO:BP	carboxylic acid catabolic process	GO:0046395	2.60E-42	72	252
6	GO:BP	small molecule catabolic process	GO:0044282	4.50E-37	80	375
7	GO:BP	respiratory electron transport chain	GO:0022904	4.00E-32	46	124
8	GO:BP	oxidative phosphorylation	GO:0006119	1.68E-30	48	148
9	GO:BP	electron transport chain	GO:0022900	7.18E-30	51	176
10	GO:BP	purine nucleotide metabolic process	GO:0006163	8.81E-29	78	463
1	GO:CC	mitochondrial matrix	GO:0005759	3.54E-128	172	487
2	GO:CC	mitochondrial inner membrane	GO:0005743	7.56E-89	141	497
3	GO:CC	mitochondrial protein-containing complex	GO:0098798	1.33E-84	112	300
4	GO:CC	oxidoreductase complex	GO:1990204	9.00E-42	53	128
5	GO:CC	respirasome	GO:0070469	1.58E-35	44	102
6	GO:CC	inner mitochondrial membrane protein complex	GO:0098800	3.94E-35	52	158
7	GO:CC	respiratory chain complex	GO:0098803	2.13E-31	39	91
8	GO:CC	mitochondrial respirasome	GO:0005746	8.67E-31	39	94
9	GO:CC	organellar ribosome	GO:0000313	2.44E-19	29	89
10	GO:CC	mitochondrial ribosome	GO:0005761	2.44E-19	29	89

Supplementary Table S10. Functional enrichment of proteins significantly modulated in MCM-activated HAMEC. Only top 10 terms included in the classification Biological Processes (BP) and Cellular Components (CC) as noted in the Gene Ontology (GO) database are listened below. Abundance changes affecting proteins annotated in categories of interest are represented in **Figure S6f**. For additional detail, see in the **Source Data file**.

#	source	term_name	term_id	adj._p-value	term_size	intersection_size
1	GO:BP	response to hydrogen peroxide	GO:0042542	3.20E-04	17	99
2	GO:BP	cellular respiration	GO:0045333	4.46E-04	27	245
3	GO:BP	RNA splicing	GO:0008380	9.09E-04	40	482
4	GO:BP	RNA splicing, via transesterification reactions	GO:0000377	1.17E-03	31	336
5	GO:BP	mRNA splicing, via spliceosome	GO:0000398	1.17E-03	31	336
6	GO:BP	RNA splicing, via transesterification reactions	GO:0000375	1.26E-03	31	340
7	GO:BP	response to reactive oxygen species	GO:0000302	1.96E-03	22	201
8	GO:BP	ribonucleoprotein complex biogenesis	GO:0022613	3.85E-03	38	494
9	GO:BP	spliceosomal complex assembly	GO:0000245	3.85E-03	14	96
10	GO:BP	energy derivation by oxidation of organic compounds	GO:0015980	4.30E-03	30	352
1	GO:CC	collagen-containing extracellular matrix	GO:0062023	1.09E-07	44	432
2	GO:CC	ribosomal subunit	GO:0044391	2.22E-06	25	186
3	GO:CC	ribosome	GO:0005840	6.41E-06	28	244
4	GO:CC	sm-like protein family complex	GO:0120114	2.03E-05	18	119
5	GO:CC	U2-type spliceosomal complex	GO:0005684	2.03E-05	16	95
6	GO:CC	spliceosomal snrnp complex	GO:0097525	2.28E-05	16	97
7	GO:CC	spliceosomal complex	GO:0005681	2.41E-05	24	208
8	GO:CC	small nuclear ribonucleoprotein complex	GO:0030532	6.29E-05	16	107
9	GO:CC	U2-type precatalytic spliceosome	GO:0071005	6.29E-05	11	50
10	GO:CC	precatalytic spliceosome	GO:0071011	8.60E-05	11	52

Supplementary Table S11. Functional enrichment of proteins significantly modulated in ACM-activated HAMEC. Abundance changes affecting proteins annotated in categories of interest are represented in **Figure S7f**. For additional details, see in the **Source Data file**.

#	source	term_name	term_id	adj._p-value	term_size	intersection_size
1	GO:BP	ribose phosphate metabolic process	GO:0019693	7.83E-09	57	379
2	GO:BP	ribonucleotide metabolic process	GO:0009259	7.83E-09	56	371
3	GO:BP	proton motive force-driven mitochondrial atp synthesis	GO:0042776	7.83E-09	22	68
4	GO:BP	proton motive force-driven atp synthesis	GO:0015986	1.12E-08	23	77
5	GO:BP	aerobic respiration	GO:0009060	1.12E-08	38	201
6	GO:BP	ATP biosynthetic process	GO:0006754	1.12E-08	26	100
7	GO:BP	nucleoside phosphate biosynthetic process	GO:1901293	1.12E-08	50	322
8	GO:BP	nucleoside triphosphate biosynthetic process	GO:0009142	1.12E-08	29	125
9	GO:BP	ribonucleoside triphosphate biosynthetic process	GO:0009201	1.12E-08	28	117
10	GO:BP	mitochondrion organization	GO:0007005	1.12E-08	61	445
1	GO:CC	respiratory chain complex	GO:0098803	1.28E-09	28	109
2	GO:CC	NADH dehydrogenase complex	GO:0030964	1.84E-08	17	46
3	GO:CC	respiratory chain complex i	GO:0045271	1.84E-08	17	46
4	GO:CC	cell-substrate junction	GO:0030055	5.64E-06	52	434
5	GO:CC	focal adhesion	GO:0005925	5.64E-06	51	424
6	GO:CC	mitochondrial protein-containing complex	GO:0098798	7.82E-06	29	178
7	GO:CC	ficolin-1-rich granule	GO:0101002	1.58E-05	29	185
8	GO:CC	oxidoreductase complex	GO:1990204	4.47E-05	25	153
9	GO:CC	ficolin-1-rich granule lumen	GO:1904813	1.79E-04	21	124
10	GO:CC	lysosomal membrane	GO:0005765	2.31E-04	48	451

Supplementary Table S12. Functional enrichment of proteins significantly modulated in adipose tissue upon WL. Only top 10 terms included in the classification Biological Processes (BP) and Cellular Components (CC) as noted in the Gene Ontology (GO) database are listened below. Abundance changes affecting proteins annotated in categories of interest are represented in **Figure 5c**. For additional details, see in the **Source Data file**, with source data underlying the plots contained in this article.

#	source	term_name	term_id	Adj._p-value	term_size	intersection_size
1	GO:BP	aerobic respiration	GO:0009060	1.46E-22	38	197
2	GO:BP	organic acid catabolic process	GO:0016054	1.46E-22	42	252
3	GO:BP	carboxylic acid catabolic process	GO:0046395	1.46E-22	42	252
4	GO:BP	cellular respiration	GO:0045333	2.62E-22	41	243
5	GO:BP	energy derivation by oxidation of organic compounds	GO:0015980	2.02E-20	45	337
6	GO:BP	small molecule catabolic process	GO:0044282	2.61E-20	47	375
7	GO:BP	nucleoside bisphosphate metabolic process	GO:0033865	1.88E-18	28	125
8	GO:BP	ribonucleoside bisphosphate metabolic process	GO:0033875	1.88E-18	28	125
9	GO:BP	purine nucleoside bisphosphate metabolic process	GO:0034032	1.88E-18	28	125
10	GO:BP	thioester metabolic process	GO:0035383	6.65E-17	24	96
1	GO:CC	mitochondrial matrix	GO:0005759	1.64E-52	85	487
2	GO:CC	mitochondrial protein-containing complex	GO:0098798	3.86E-32	53	300
3	GO:CC	oxidoreductase complex	GO:1990204	1.48E-26	34	128
4	GO:CC	mitochondrial inner membrane	GO:0005743	1.48E-26	59	497
5	GO:CC	tricarboxylic acid cycle enzyme complex	GO:0045239	5.91E-12	10	16
6	GO:CC	inner mitochondrial membrane protein complex	GO:0098800	7.15E-11	22	158
7	GO:CC	mitochondrial pyruvate dehydrogenase complex	GO:0005967	5.23E-10	7	8
8	GO:CC	pyruvate dehydrogenase complex	GO:0045254	5.23E-10	7	8
9	GO:CC	respirasome	GO:0070469	9.91E-10	17	102
10	GO:CC	cytochrome complex	GO:0070069	1.02E-09	12	42

SUPPLEMENTARY FIGURE LEGENDS

Supplementary Figure S1. (a) Numbers of identified proteins in ex vivo isolated adipocyte samples obtained from gallstone surgery patients with (BMI>30 kg/m^2) and without (BMI<25 kg/m^2) obesity (n=5 and 3, respectively). **(b)** Plotted Log_2-scale intensities (log2maxlfq) of identified proteins. **(c)** Hierarchical clustering. **(d)** GSEA (Reactome) of proteomic results in "obese" vs "lean" adipocytes.

Supplementary Figure S2. (a) Plotted Log_2-scale intensities (log2maxlfq) of metabolites as quantified in isolated adipocyte samples from gallstone surgery patients with (BMI>30 kg/m^2) and without (BMI<25 kg/m^2) obesity (n=8 and 9, respectively). **(b)** Correlation heatmap. **(c)** PCA analysis and **(d)** heatmap of log2maxlfq values. **(e)** ORA (KEGG) and pathway interpretation of metabolomic results in "obese" vs "lean" adipocytes.

Supplementary Figure S3. (a) Numbers of identified proteins in ex vivo isolated endothelial cell (EC) samples obtained from gallstone surgery patients with (BMI>30 kg/m^2) and without (BMI<25 kg/m^2) obesity (n=5 and 7, respectively). **(b)** Plotted Log_2-scale intensities (log2maxlfq) of identified proteins. **(c)** Hierarchical clustering. **(d)** GSEA (Reactome) of proteomic results in "obese" vs "lean" EC.

Supplementary Figure S4. (a) Numbers of identified proteins in primary human preadipocyte cultures. **(b)** Plotted Log_2-scale intensities (log2maxlfq) of identified proteins, and **(c)** hierarchical clustering of preadipocytes (PA) and mature adipocytes (MA) samples (n=4/group). **(d)** Hierarchical clustering of cultures of MA when treated with 1% MCM for 72 hours and controls (n=4/group). **(e)** Numbers of identified proteins, and **(f)** plotted Log_2-scale intensities (log2maxlfq) in inflamed adipocytes (MCM) and controls (CTRL). **(g)** Seahorse mitochondrial stress flux analysis and measures of oxygen consumption rate (OCR) obtained in MA cultures when treated with 1% MCM or vehicle (CTRL) for 72 h (3 assays/each). (**1**) Spare respiratory capacity, (**2**) maximal, (**3**) basal, and (**4**) ATP-production coupled respiration, and (**5**) non-mitochondrial oxygen consumption. The significance was calculated by means of the Mann-Whitney test (Holm-Šídák method for multiple comparisons). *p<0.05, **p<0.01, ***p<0.001.

Supplementary Figure S5. (a) Multivariable analysis (PCA) shows the clustering of primary human preadipocyte cultures (n=4/group) upon differentiation into MA and when maintained under basal culture conditions without hormonal stimuli (PA). **(b)** The volcano plot shows DAPs up (red) and down-regulated (blue) in differentiated adipocytes vs PA. Statistical significance was assessed by employing two-tailed Bayesian moderated t-tests and assuming equal variance in unpaired comparisons, and dots in grey show proteins meeting our exclusion criteria (nominal p-value≥0.05). Colored labels indicate protein landmarks of Gene ontology (GO) pathways significantly regulated after adipocyte differentiation, i.e., golgi-vesicle transport (GO:0048193), cell-substrate junction (GO:0030055), cellular respiration (GO:0045333), oxidative phosphorylation (GO:0006119), fatty acid metabolism (GO:0006631), fatty acid beta-oxidation (GO:0006635), and branched-chain amino acid metabolism (GO:0009081). **(c)** Bubble plots created by applying Over-representation analysis (ORA) to enrichment terms in a GO computational framework. ORA pathways were segregated in Biological processes (BP) and Cellular components (CC). Additional details are provided in **Table**

S8. **(d)** Gene set enrichment analysis (GSEA) and Kyoto encyclopedia of genes and genomes (KEGG) annotations showed, as expected, the upregulation of cellular processes related to carbon and fatty acid metabolism. **(e)** Lipidomes conducted in PA (n=3) and MA (n=3) showed the higher presence of many glycerophospholipid and sphingolipid species. The dynamic nature of lipids in fat precursor cells upon adipogenic transformation pointed at the modulation of triglycerides (TG), sphingomyelins (SM), phosphatidylserines (PS), phosphatidylinositols (PI), phosphatidylglycerols (PG), phosphatidylethanolamines (PE), phosphatidylcholines (PC), phosphatidic acids (PA), lyso-glycerophosphatidylethanolamines (LPE) and lysophosphatidylcholines (LPC), hexosylceramides (HexCer), free cholesterols (FC), diglycerides (DG), cardiolipins (CL), ceramides (Cer), and cholesteryl esters (CE). Bubble plot in **(f)** shows modulation of TG species, segregated according to the saturation (nº double bonds) and main length (nº carbon atoms) of FA. Lipid concentrations were normalized based on the total amount within each lipid class, followed by log_2 transformation for conducting two-tailed Student's t-test between study and control group. Differential abundance of lipids was identified based on an absolute log_2 fold-change (FC) value$\geq$0.58 and p-value<0.05. Source data are provided as a **Source data file** for **Figures S5c** and **S5d**.

Supplementary Figure S6. (a) Numbers of identified proteins in HAMEC cultures upon treatment with LPS-conditioned macrophage media (MCM) vs control (vehicle), n=4/group. **(b)** Plotted Log_2-scale intensities (log2maxlfq) of identified proteins, and **(c)** correlation heatmap. **(d)** PCA of proteomics results in 1% MCM-activated HAMEC. **(e)** The volcano plot shows DAPs up (red) and down-regulated (blue) in MCM-activated HAMEC. Statistical significance was assessed by employing two-tailed Bayesian moderated t-tests and assuming equal variance in unpaired comparisons, and dots in grey show proteins meeting our exclusion criteria (nominal p-value$\geq$0.05). Colored labels point at protein landmarks of Hallmark pathways significantly regulated in activated EC. **(f)** ORA enrichment terms in a GO computational framework. **(g)** GSEA (Hallmark) annotations according to the main function of altered significantly protein hubs. Source data are provided as a **Source data file**.

Supplementary Figure S7. (a) Numbers of identified proteins in HAMEC cultures upon treatment with MCM-conditioned adipocyte media (ACM) vs control (vehicle), n=4/group. **(b)** Plotted Log_2-scale intensities (log2maxlfq) of identified proteins, and **(c)** correlation heatmap. **(d)** PCA of proteomics results in 10% ACM-activated HAMEC. **(e)** The volcano plot shows DAPs up (red) and down-regulated (blue) in ACM-activated HAMEC. Statistical significance was assessed by employing two-tailed Bayesian moderated t-tests and assuming equal variance in unpaired comparisons. Dots in grey show proteins meeting our exclusion criteria (nominal p-value $\geq$ 0.05). Colored labels point at protein landmarks of Hallmark pathways significantly regulated in activated EC. **(f)** ORA enrichment terms in a GO computational framework. **(g)** GSEA (Hallmark) annotations according to the main function of significantly altered protein hubs. Source data are provided as a **Source data file**.

Supplementary Figure S8. In bulk adipose tissue before-after surgery-induced weight loss, **(a)** number of identified protein groups per sample after filtering out peptides without replication within subgroups and proteins with less than 2 peptides. **(b)** Plotted Log_2-scale intensities (log2maxlfq). **(c)** Hierarchical clustering of proteins abundance (in rows) for each sample (in columns). **(d)** GSEA of

proteomic results and pathway interpretation according to the Reactome database by comparing post-weight loss proteomes with baseline proteomes.

Supplementary Figure S9. Integrative heatmap of lipidomic results including lipids that were conjointly regulated in two or more of our experimental approaches, i.e., **(a)** in vitro (inflamed adipocyte cultures), **(b)** ex vivo ("obese" vs "lean" adipocytes), and/or **(c)** in vivo (bulk adipose tissue after successful weight loss).

Supplementary Figure S10. Flowchart study design diagram showing **(a)** results in adipocytes and bulk adipose tissue, and **(b)** gene candidate confirmation in bulk adipose tissue transcriptomes from three large cross-sectional datasets (METSIM, Finish Twin Cohort, and ADIPOMIT). Red squares depict proteins/genes increased. Blue squares for proteins/genes decreased.

Supplementary Figure S11. Flowchart study design diagram showing **(a)** proteomic results in adipose microvascular EC and HAMEC cultures when challenged with MCM and ACM. Then, gene candidates were leveraged with multiple pre-post surgery induced weight loss transcriptomes in bulk fat, filtered and merged with those from adipocyte proteomes. **(b)** Gene candidate-metabolic trait assessment was conducted by means of ssGSEA, ROC analyses, and machine learning in ADIPOMIT and KOBS cross-sectional transcriptomes. Red squares depict proteins/genes increased. Blue squares for proteins/genes decreased.

Supplementary Figure S12. (a) Integration of protein datasets obtained in ex vivo isolated "obese" vs "lean" adipose-resident EC and in vitro cultures of MCM and ACM-activated HAMEC when compared to control. **(b)** GO annotations of genes highlighted during our research (32) revealed regulation of several ribosomal components, and translation-related and biosynthetic processes. **(c)** Gene concept network depicting the relationship within these 32 genes/proteins. The Markov Cluster Algorithm (MCL) was used to find natural clusters based on the stochastic flow (inflation parameter: 3). Pathways with the same color correspond to the same cluster. Line thickness indicates the strength of data support. Dotted lines show edges between clusters. **(d)** The violin plot shows the ability of this EC-specific gene cluster in segregating "healthy" (HO) and "unhealthy" (UO) obesity. Group 1 to 3 indicate the number of metabolic comorbidities (i.e., dyslipidemia, hypertriglyceridemia, and/or hyperglycemia) observed, together with obesity in the ADIPOMIT cohort. **(e)** Combination of adipocyte and adipose-resident EC-specific protein biomarkers, as assessed after meta-analysis and translational cross-evaluation. Notably, only Thrombospondin 1 (THBS1) and Biphenyl hydrolase like (BPHL) proteins were underlined in adipocytes and EC samples.

Supplementary Figure S13. Bar plots feature variable importance rankings across 6 machine learning algorithms (i.e., logistic regression, random forest, decision tree, support vector machine (SVM), LightGBM, and XGBoost) for the diagnosis of obesity-related disturbances and "healthy" (HO) and "unhealthy" (UO) obesity in **(a)** ADIPOMIT and **(b)** KOBS. Each bar represents the normalized score assigned to a given variable within each model. Labels in blue for EC-derived genes. Below, **(c)** Venn diagrams depict gene coincidences across datasets and algorithms taken two-by-two (i.e., logistic regression and random forest, decision tree and SVM, and LightGBM and XGBoost). Source data are provided as a **Source data file**.

Figure S1 (Chaurasiya *et al.*)

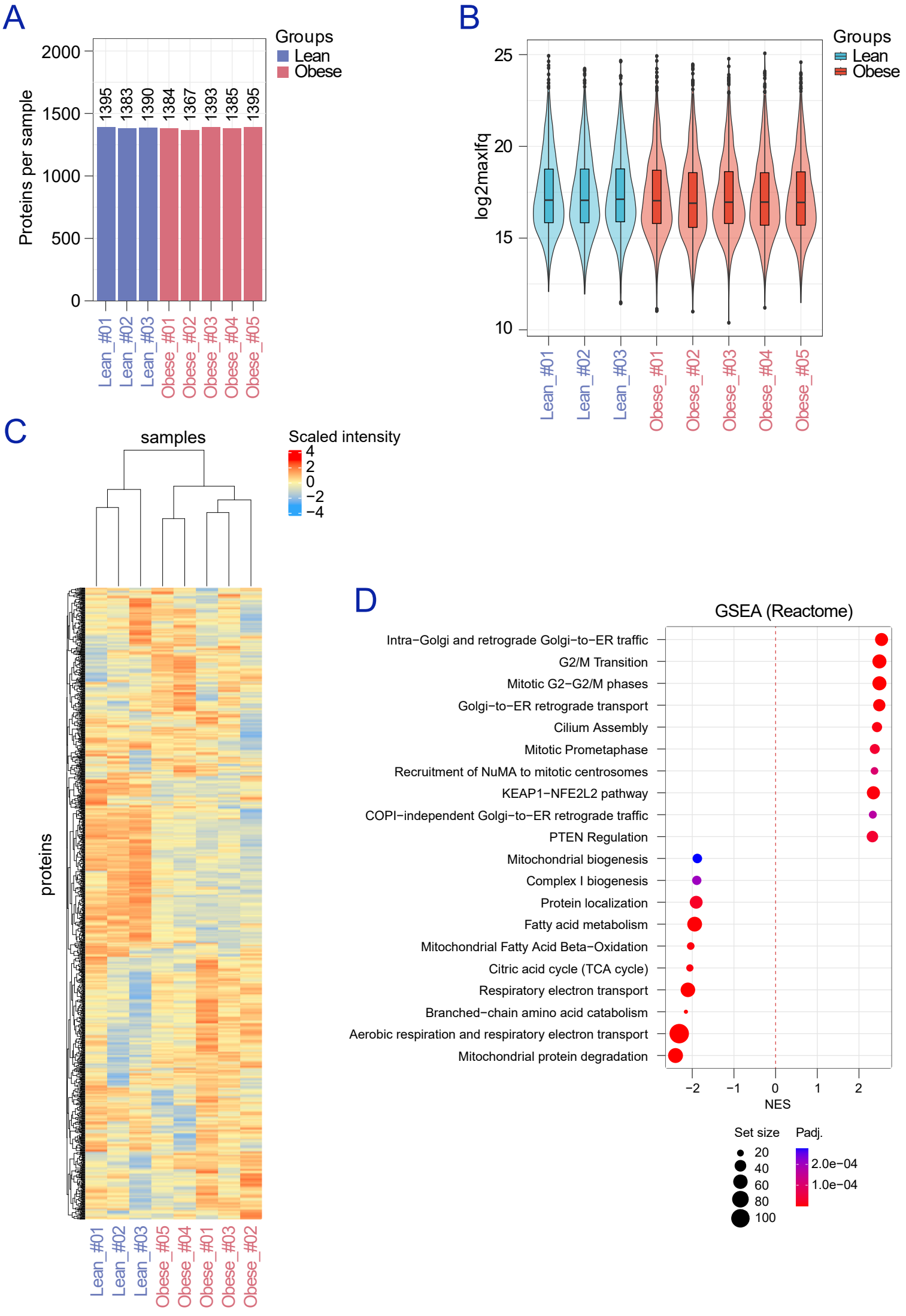

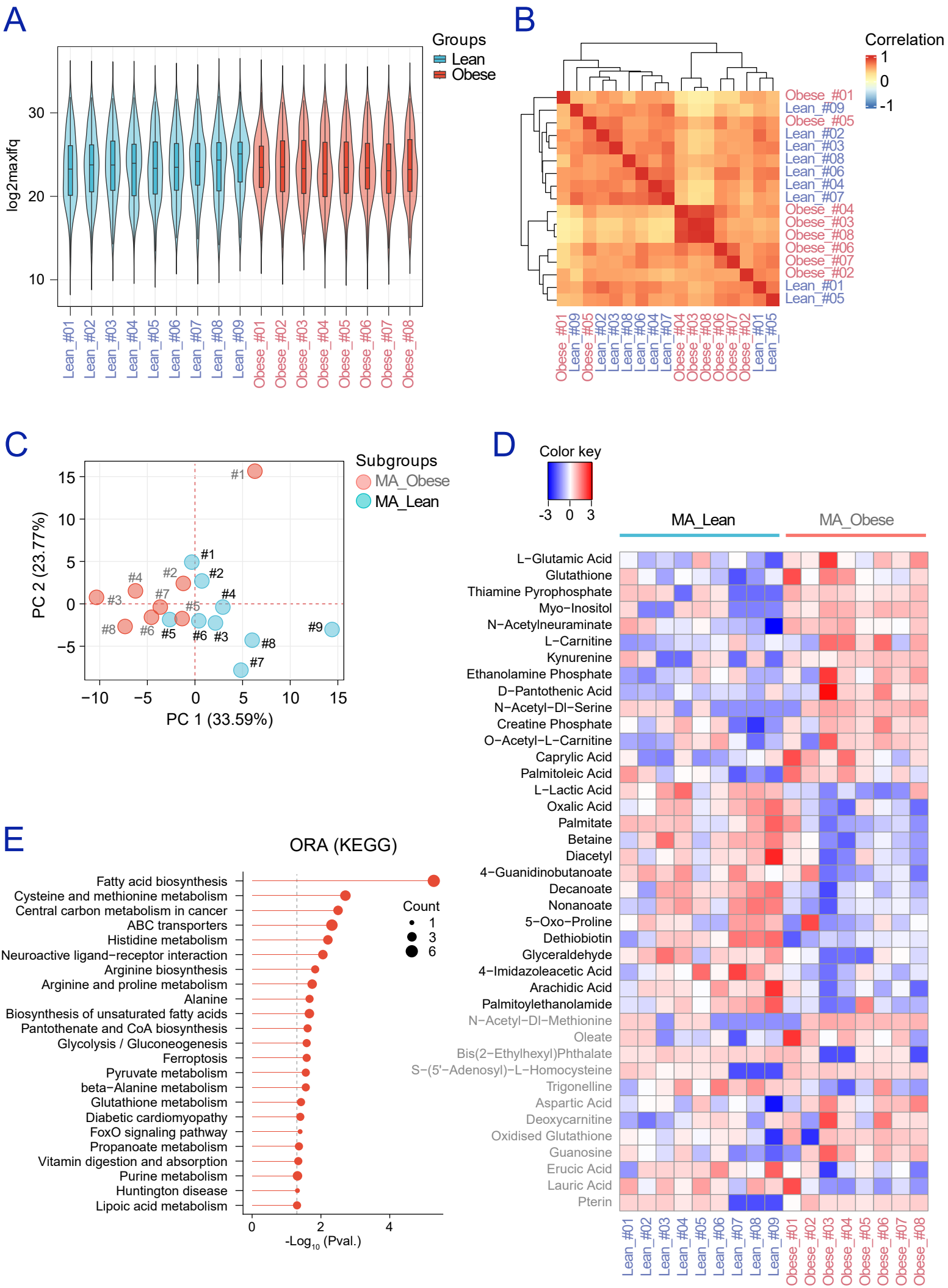
A
Groups
Lean
Obese
log2maxlfq
30
20
10
Lean_#01
Lean_#02
Lean_#03
Lean_#04
Lean_#05
Lean_#06
Lean_#07
Lean_#08
Lean_#09
Obese_#01
Obese_#02
Obese_#03
Obese_#04
Obese_#05
Obese_#06
Obese_#07
Obese_#08
B
Correlation
1
0
-1
Obese_#01
Lean_#09
Obese_#05
Lean_#02
Lean_#03
Lean_#08
Lean_#06
Lean_#04
Lean_#07
Obese_#04
Obese_#03
Obese_#08
Obese_#06
Obese_#07
Obese_#02
Lean_#01
Lean_#05
C
Subgroups
MA_Obese
MA_Lean
PC 2 (23.77%)
PC 1 (33.59%)
15
10
5
0
−5
−10
−5
0
5
10
15
#1
#2
#3
#4
#5
#6
#7
#8
#9
D
Color key
-3
0
3
MA_Lean
MA_Obese
L−Glutamic Acid
Glutathione
Thiamine Pyrophosphate
Myo−Inositol
N−Acetylneuraminate
L−Carnitine
Kynurenine
Ethanolamine Phosphate
D−Pantothenic Acid
N−Acetyl−Dl−Serine
Creatine Phosphate
O−Acetyl−L−Carnitine
Caprylic Acid
Palmitoleic Acid
L−Lactic Acid
Oxalic Acid
Palmitate
Betaine
Diacetyl
4−Guanidinobutanoate
Decanoate
Nonanoate
5−Oxo−Proline
Dethiobiotin
Glyceraldehyde
4−Imidazoleacetic Acid
Arachidic Acid
Palmitoylethanolamide
N−Acetyl−Dl−Methionine
Oleate
Bis(2−Ethylhexyl)Phthalate
S−(5'−Adenosyl)−L−Homocysteine
Trigonelline
Aspartic Acid
Deoxycarnitine
Oxidised Glutathione
Guanosine
Erucic Acid
Lauric Acid
Pterin
Lean_#01
Lean_#02
Lean_#03
Lean_#04
Lean_#05
Lean_#06
Lean_#07
Lean_#08
Lean_#09
Obese_#01
Obese_#02
Obese_#03
Obese_#04
Obese_#05
Obese_#06
Obese_#07
Obese_#08
E
ORA (KEGG)
Fatty acid biosynthesis
Cysteine and methionine metabolism
Central carbon metabolism in cancer
ABC transporters
Histidine metabolism
Neuroactive ligand−receptor interaction
Arginine biosynthesis
Arginine and proline metabolism
Alanine
Biosynthesis of unsaturated fatty acids
Pantothenate and CoA biosynthesis
Glycolysis / Gluconeogenesis
Ferroptosis
Pyruvate metabolism
beta−Alanine metabolism
Glutathione metabolism
Diabetic cardiomyopathy
FoxO signaling pathway
Propanoate metabolism
Vitamin digestion and absorption
Purine metabolism
Huntington disease
Lipoic acid metabolism
Count
1
3
6
0
2
4
-Log10 (Pval.)

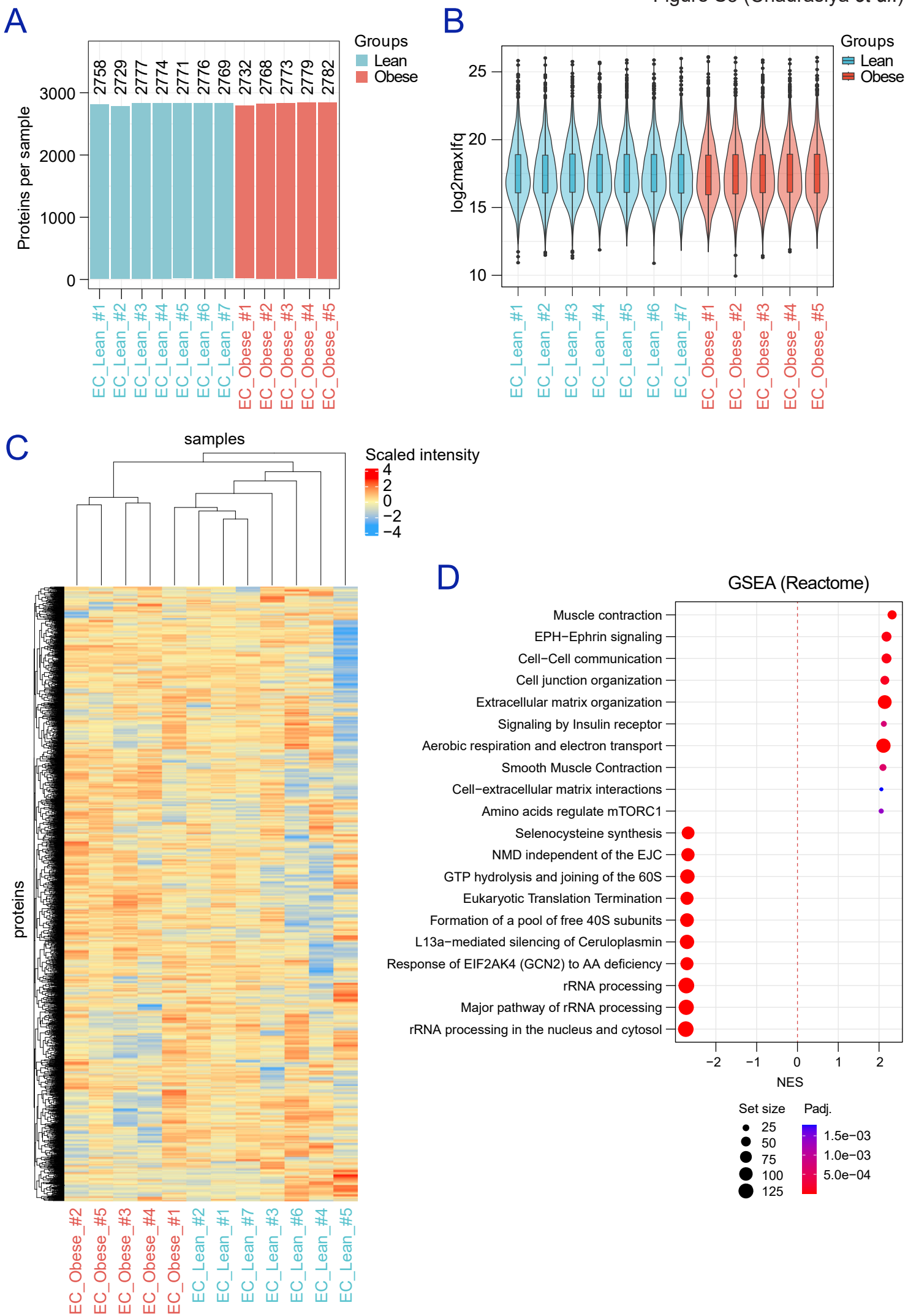
A
Groups
Lean
Obese
Proteins per sample
0
1000
2000
3000
2758
2729
2777
2774
2771
2776
2769
2732
2768
2773
2779
2782
EC_Lean_#1
EC_Lean_#2
EC_Lean_#3
EC_Lean_#4
EC_Lean_#5
EC_Lean_#6
EC_Lean_#7
EC_Obese_#1
EC_Obese_#2
EC_Obese_#3
EC_Obese_#4
EC_Obese_#5
B
Groups
Lean
Obese
log2maxlfq
10
15
20
25
C
samples
Scaled intensity
4
2
0
−2
−4
proteins
EC_Obese_#2
EC_Obese_#5
EC_Obese_#3
EC_Obese_#4
EC_Obese_#1
EC_Lean_#2
EC_Lean_#1
EC_Lean_#7
EC_Lean_#3
EC_Lean_#6
EC_Lean_#4
EC_Lean_#5
D
GSEA (Reactome)
Muscle contraction
EPH−Ephrin signaling
Cell−Cell communication
Cell junction organization
Extracellular matrix organization
Signaling by Insulin receptor
Aerobic respiration and electron transport
Smooth Muscle Contraction
Cell−extracellular matrix interactions
Amino acids regulate mTORC1
Selenocysteine synthesis
NMD independent of the EJC
GTP hydrolysis and joining of the 60S
Eukaryotic Translation Termination
Formation of a pool of free 40S subunits
L13a−mediated silencing of Ceruloplasmin
Response of EIF2AK4 (GCN2) to AA deficiency
rRNA processing
Major pathway of rRNA processing
rRNA processing in the nucleus and cytosol
−2
−1
0
1
2
NES
Set size
25
50
75
100
125
Padj.
1.5e−03
1.0e−03
5.0e−04

Figure S4 (Chaurasiya *et al.*)

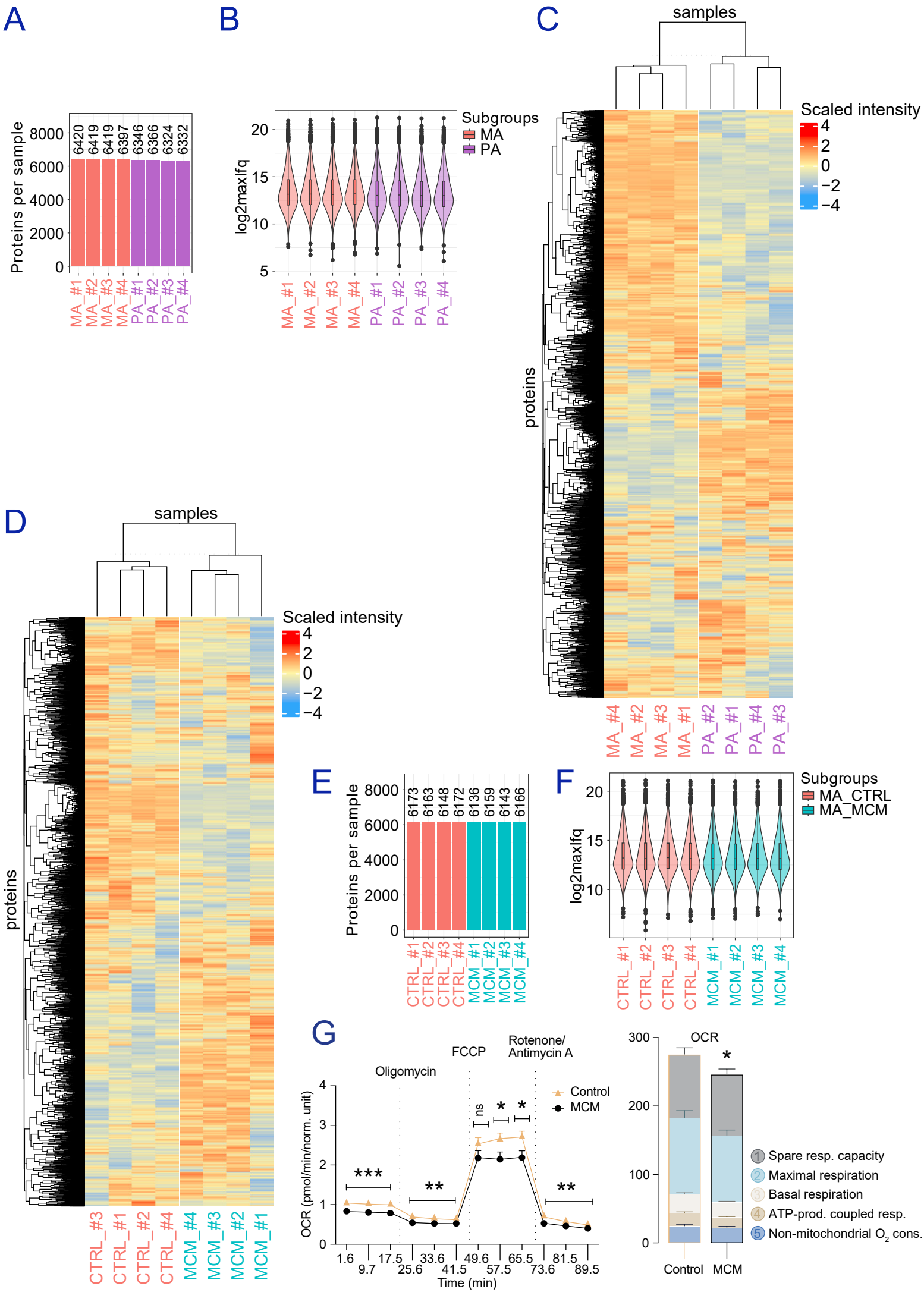

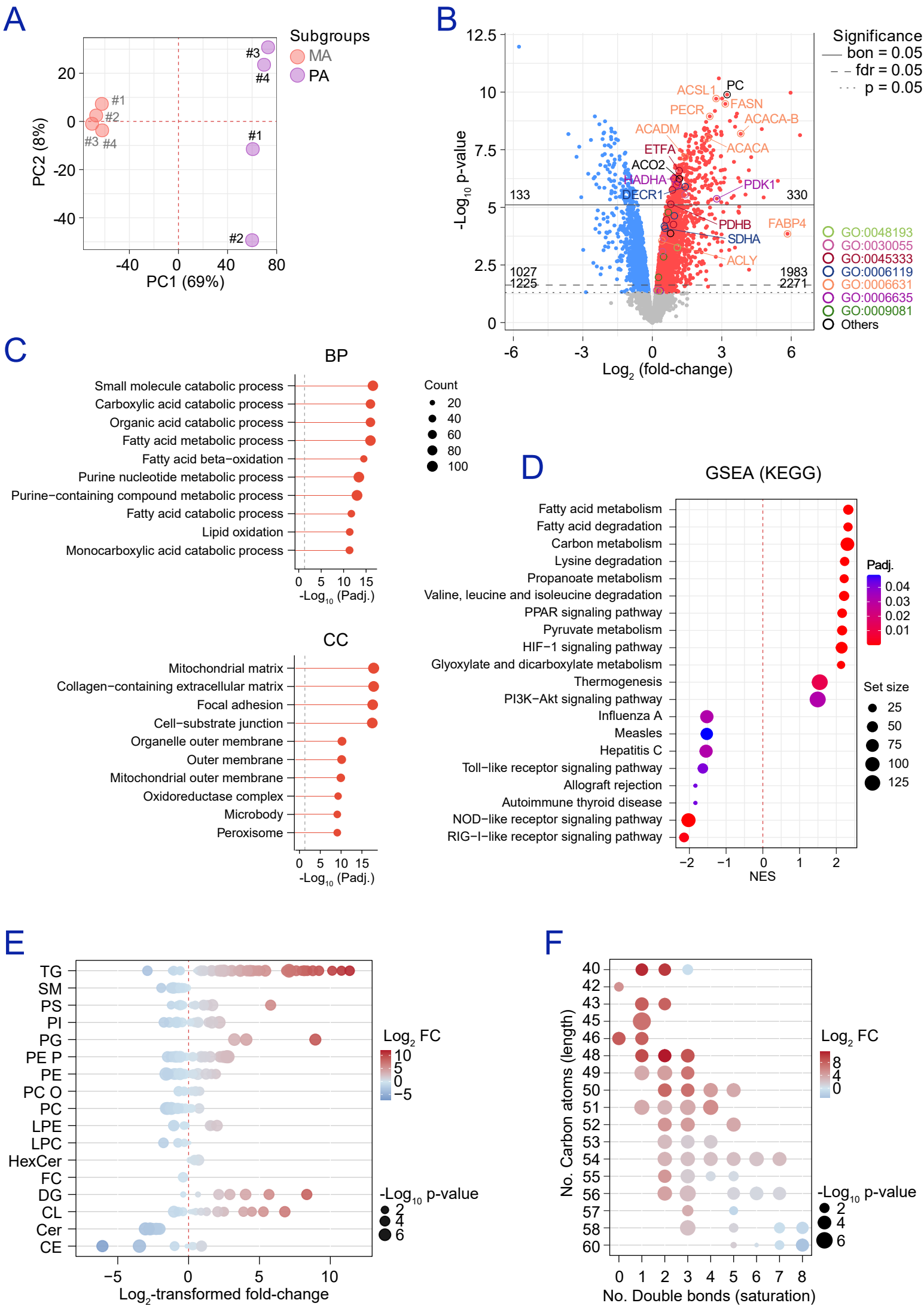
A
Subgroups
MA
PA
#1
#2
#3
#4
PC2 (8%)
PC1 (69%)
B
Significance
bon = 0.05
fdr = 0.05
p = 0.05
ACSL1
PC
PECR
FASN
ACACA-B
ACADM
ACACA
ETFA
ACO2
HADHA
PDK1
ECR1
PDHB
FABP4
SDHA
ACLY
133
330
1027
1225
1983
2271
-Log10 p-value
Log2 (fold-change)
GO:0048193
GO:0030055
GO:0045333
GO:0006119
GO:0006631
GO:0006635
GO:0009081
Others
C
BP
Small molecule catabolic process
Carboxylic acid catabolic process
Organic acid catabolic process
Fatty acid metabolic process
Fatty acid beta−oxidation
Purine nucleotide metabolic process
Purine−containing compound metabolic process
Fatty acid catabolic process
Lipid oxidation
Monocarboxylic acid catabolic process
Count
-Log10 (Padj.)
CC
Mitochondrial matrix
Collagen−containing extracellular matrix
Focal adhesion
Cell−substrate junction
Organelle outer membrane
Outer membrane
Mitochondrial outer membrane
Oxidoreductase complex
Microbody
Peroxisome
D
GSEA (KEGG)
Fatty acid metabolism
Fatty acid degradation
Carbon metabolism
Lysine degradation
Propanoate metabolism
Valine, leucine and isoleucine degradation
PPAR signaling pathway
Pyruvate metabolism
HIF−1 signaling pathway
Glyoxylate and dicarboxylate metabolism
Thermogenesis
PI3K−Akt signaling pathway
Influenza A
Measles
Hepatitis C
Toll−like receptor signaling pathway
Allograft rejection
Autoimmune thyroid disease
NOD−like receptor signaling pathway
RIG−I−like receptor signaling pathway
Padj.
Set size
NES
E
TG
SM
PS
PI
PG
PE P
PE
PC O
PC
LPE
LPC
HexCer
FC
DG
CL
Cer
CE
Log2 FC
-Log10 p-value
Log2-transformed fold-change
F
No. Carbon atoms (length)
No. Double bonds (saturation)
Log2 FC
-Log10 p-value

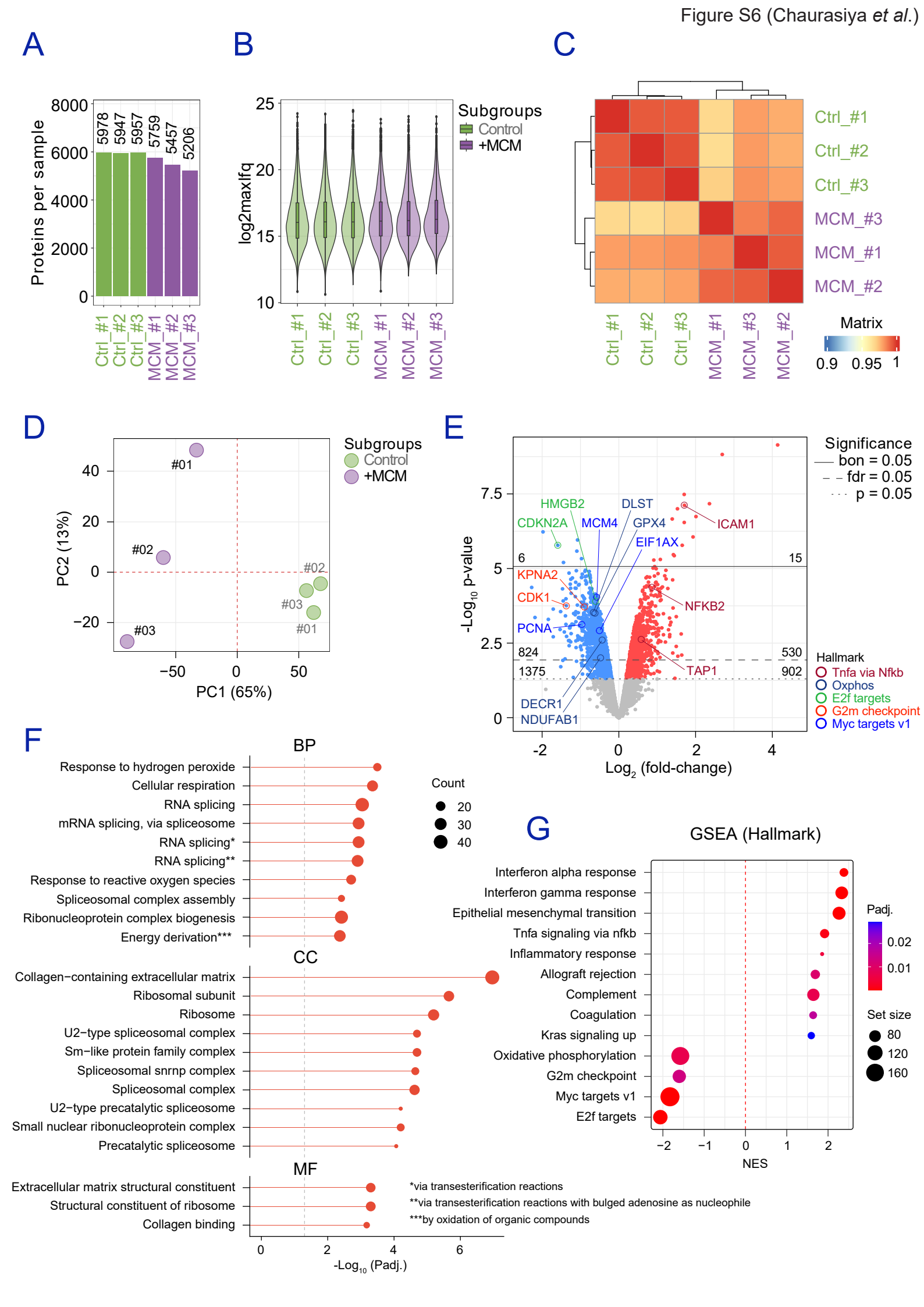
A
Proteins per sample
8000
6000
4000
2000
0
5978
5947
5957
5759
5457
5206
Ctrl_#1
Ctrl_#2
Ctrl_#3
MCM_#1
MCM_#2
MCM_#3
B
log2maxlfq
25
20
15
10
Subgroups
Control
+MCM
C
Ctrl_#1
Ctrl_#2
Ctrl_#3
MCM_#3
MCM_#1
MCM_#2
Matrix
0.9
0.95
1
D
PC2 (13%)
PC1 (65%)
#01
#02
#03
Subgroups
Control
+MCM
E
-Log10 p-value
Log2 (fold-change)
Significance
bon = 0.05
fdr = 0.05
p = 0.05
HMGB2
CDKN2A
MCM4
DLST
GPX4
EIF1AX
ICAM1
KPNA2
CDK1
PCNA
NFKB2
TAP1
DECR1
NDUFAB1
6
15
824
530
1375
902
Hallmark
Tnfa via Nfkb
Oxphos
E2f targets
G2m checkpoint
Myc targets v1
F
BP
Response to hydrogen peroxide
Cellular respiration
RNA splicing
mRNA splicing, via spliceosome
RNA splicing*
RNA splicing**
Response to reactive oxygen species
Spliceosomal complex assembly
Ribonucleoprotein complex biogenesis
Energy derivation***
Count
20
30
40
CC
Collagen−containing extracellular matrix
Ribosomal subunit
Ribosome
U2−type spliceosomal complex
Sm−like protein family complex
Spliceosomal snrnp complex
Spliceosomal complex
U2−type precatalytic spliceosome
Small nuclear ribonucleoprotein complex
Precatalytic spliceosome
MF
Extracellular matrix structural constituent
Structural constituent of ribosome
Collagen binding
-Log10 (Padj.)
*via transesterification reactions
**via transesterification reactions with bulged adenosine as nucleophile
***by oxidation of organic compounds
G
GSEA (Hallmark)
Interferon alpha response
Interferon gamma response
Epithelial mesenchymal transition
Tnfa signaling via nfkb
Inflammatory response
Allograft rejection
Complement
Coagulation
Kras signaling up
Oxidative phosphorylation
G2m checkpoint
Myc targets v1
E2f targets
NES
Padj.
0.02
0.01
Set size
80
120
160

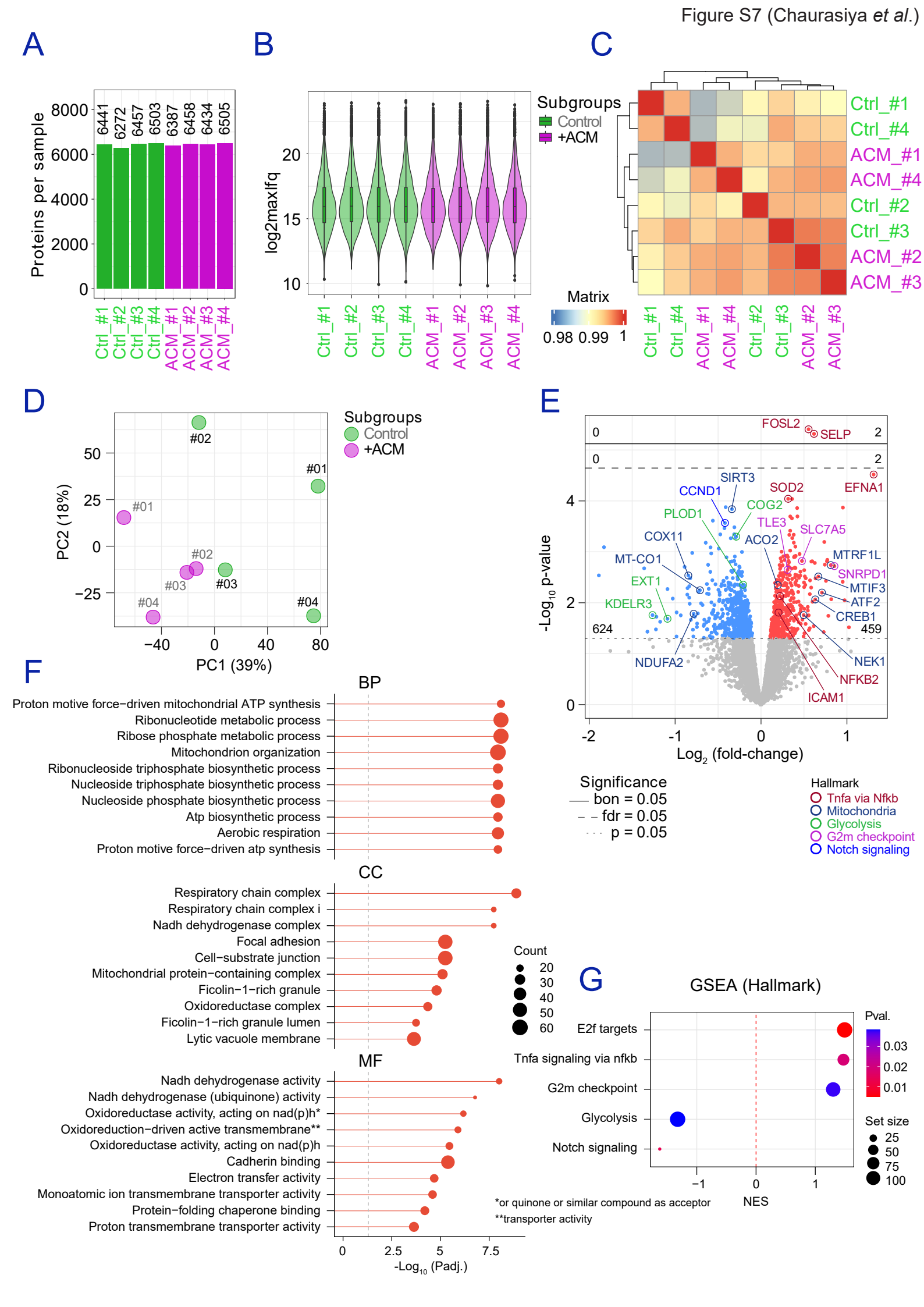
A
Proteins per sample
8000
6000
4000
2000
0
6441
6272
6457
6503
6387
6458
6434
6505
Ctrl_#1
Ctrl_#2
Ctrl_#3
Ctrl_#4
ACM_#1
ACM_#2
ACM_#3
ACM_#4
B
log2maxlfq
20
15
10
Subgroups
Control
+ACM
C
Matrix
0.98 0.99 1
D
PC2 (18%)
PC1 (39%)
50
25
0
−25
−40
0
40
80
#01
#02
#03
#04
E
-Log10 p-value
Log2 (fold-change)
FOSL2
SELP
EFNA1
SIRT3
CCND1
SOD2
COG2
PLOD1
TLE3
SLC7A5
COX11
ACO2
MTRF1L
MT-CO1
SNRPD1
EXT1
MTIF3
KDELR3
ATF2
CREB1
624
459
NDUFA2
NEK1
NFKB2
ICAM1
Significance
bon = 0.05
fdr = 0.05
p = 0.05
Hallmark
Tnfa via Nfkb
Mitochondria
Glycolysis
G2m checkpoint
Notch signaling
F
BP
Proton motive force−driven mitochondrial ATP synthesis
Ribonucleotide metabolic process
Ribose phosphate metabolic process
Mitochondrion organization
Ribonucleoside triphosphate biosynthetic process
Nucleoside triphosphate biosynthetic process
Nucleoside phosphate biosynthetic process
Atp biosynthetic process
Aerobic respiration
Proton motive force−driven atp synthesis
CC
Respiratory chain complex
Respiratory chain complex i
Nadh dehydrogenase complex
Focal adhesion
Cell−substrate junction
Mitochondrial protein−containing complex
Ficolin−1−rich granule
Oxidoreductase complex
Ficolin−1−rich granule lumen
Lytic vacuole membrane
MF
Nadh dehydrogenase activity
Nadh dehydrogenase (ubiquinone) activity
Oxidoreductase activity, acting on nad(p)h*
Oxidoreduction−driven active transmembrane**
Oxidoreductase activity, acting on nad(p)h
Cadherin binding
Electron transfer activity
Monoatomic ion transmembrane transporter activity
Protein−folding chaperone binding
Proton transmembrane transporter activity
0
2.5
5
7.5
-Log10 (Padj.)
Count
20
30
40
50
60
*or quinone or similar compound as acceptor
**transporter activity
G
GSEA (Hallmark)
E2f targets
Tnfa signaling via nfkb
G2m checkpoint
Glycolysis
Notch signaling
−1
0
1
NES
Pval.
0.03
0.02
0.01
Set size
25
50
75
100

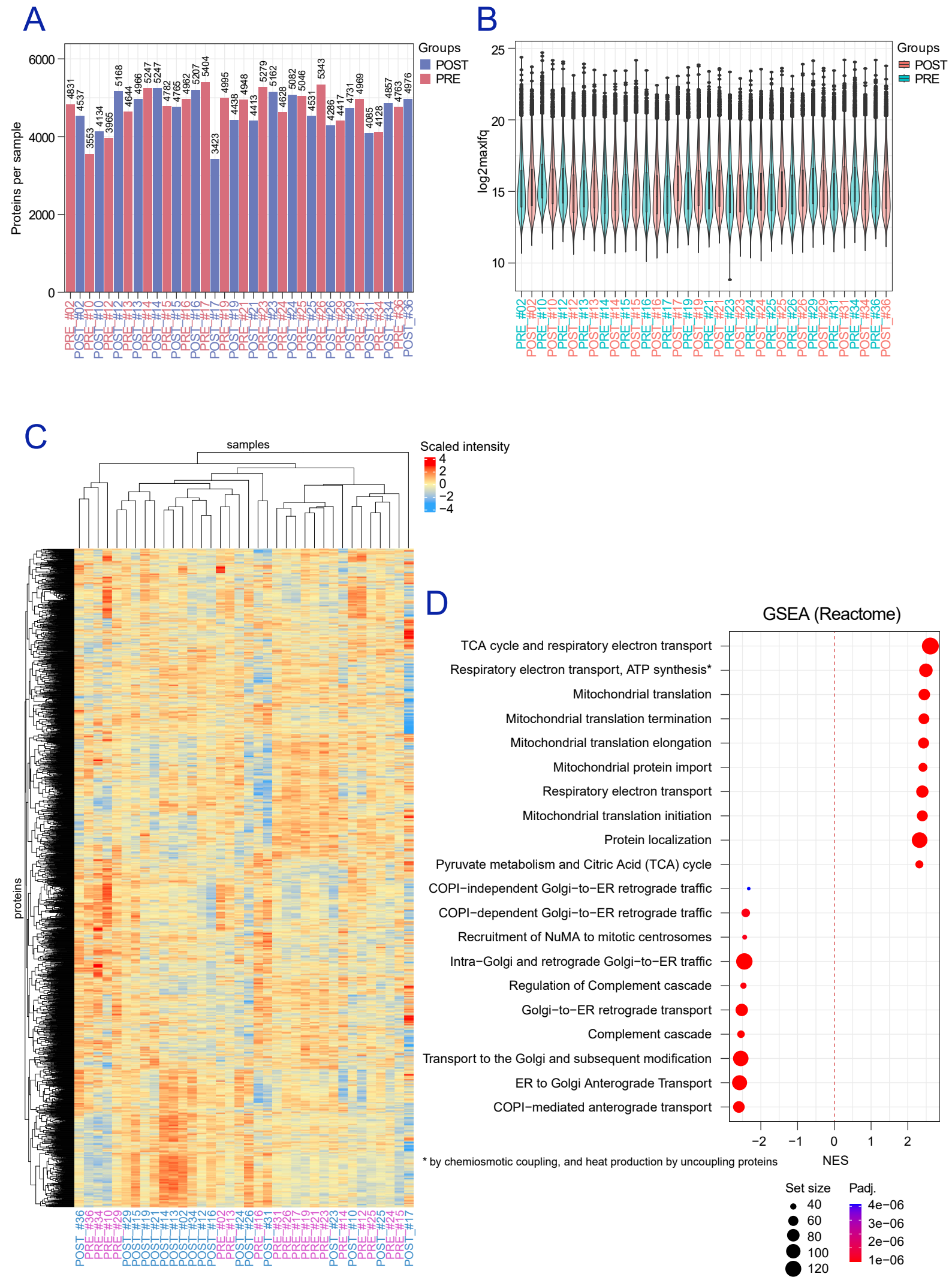
A
Proteins per sample
Groups
POST
PRE
B
log2maxlfq
Groups
POST
PRE
C
samples
Scaled intensity
proteins
D
GSEA (Reactome)
TCA cycle and respiratory electron transport
Respiratory electron transport, ATP synthesis*
Mitochondrial translation
Mitochondrial translation termination
Mitochondrial translation elongation
Mitochondrial protein import
Respiratory electron transport
Mitochondrial translation initiation
Protein localization
Pyruvate metabolism and Citric Acid (TCA) cycle
COPI−independent Golgi−to−ER retrograde traffic
COPI−dependent Golgi−to−ER retrograde traffic
Recruitment of NuMA to mitotic centrosomes
Intra−Golgi and retrograde Golgi−to−ER traffic
Regulation of Complement cascade
Golgi−to−ER retrograde transport
Complement cascade
Transport to the Golgi and subsequent modification
ER to Golgi Anterograde Transport
COPI−mediated anterograde transport
* by chemiosmotic coupling, and heat production by uncoupling proteins
NES
Set size
Padj.

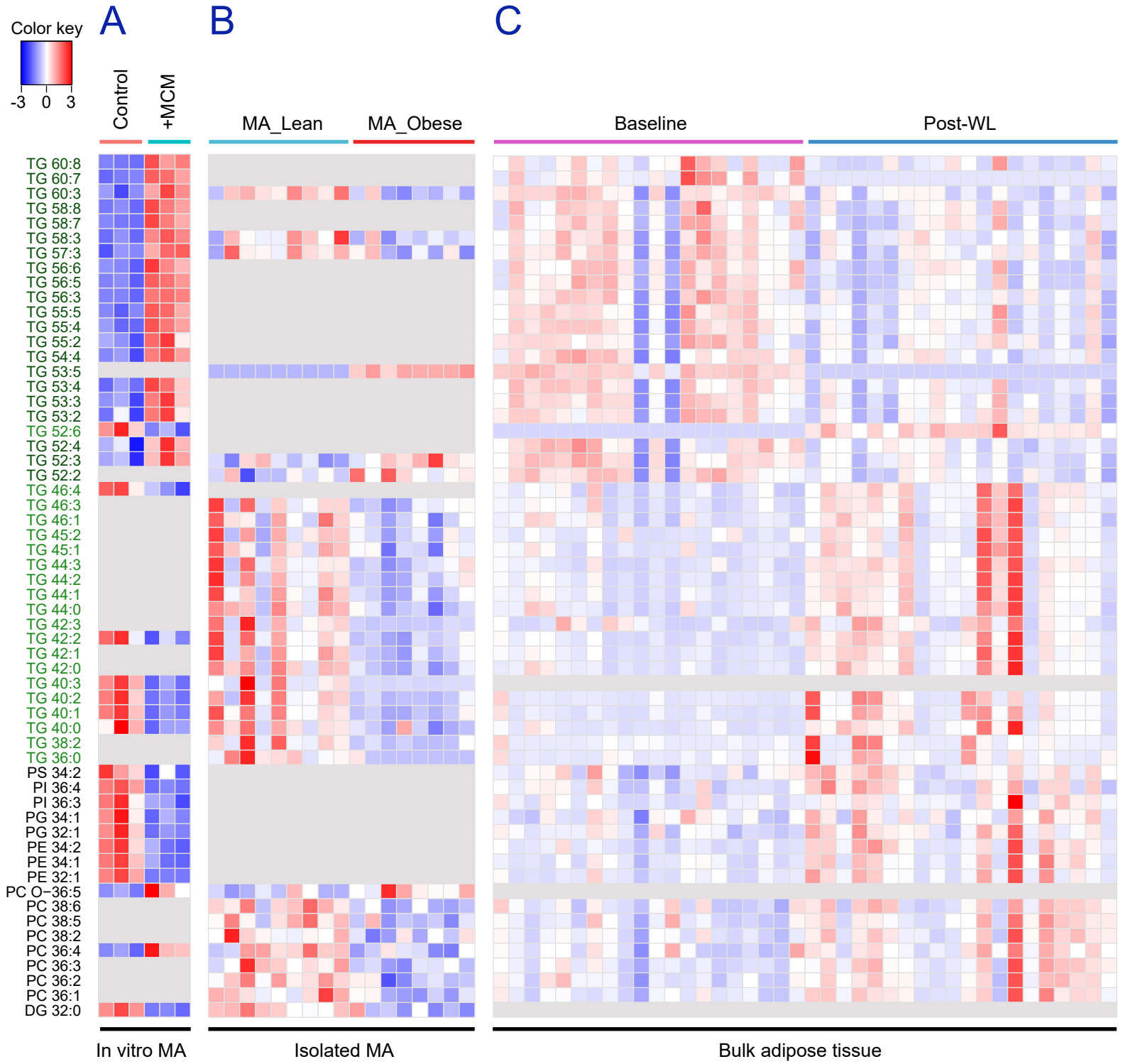
Color key
-3 0 3
A
B
C
Control
+MCM
MA_Lean
MA_Obese
Baseline
Post-WL
TG 60:8
TG 60:7
TG 60:3
TG 58:8
TG 58:7
TG 58:3
TG 57:3
TG 56:6
TG 56:5
TG 56:3
TG 55:5
TG 55:4
TG 55:2
TG 54:4
TG 53:5
TG 53:4
TG 53:3
TG 53:2
TG 52:6
TG 52:4
TG 52:3
TG 52:2
TG 46:4
TG 46:3
TG 46:1
TG 45:2
TG 45:1
TG 44:3
TG 44:2
TG 44:1
TG 44:0
TG 42:3
TG 42:2
TG 42:1
TG 42:0
TG 40:3
TG 40:2
TG 40:1
TG 40:0
TG 38:2
TG 36:0
PS 34:2
PI 36:4
PI 36:3
PG 34:1
PG 32:1
PE 34:2
PE 34:1
PE 32:1
PC O−36:5
PC 38:6
PC 38:5
PC 38:2
PC 36:4
PC 36:3
PC 36:2
PC 36:1
DG 32:0
In vitro MA
Isolated MA
Bulk adipose tissue

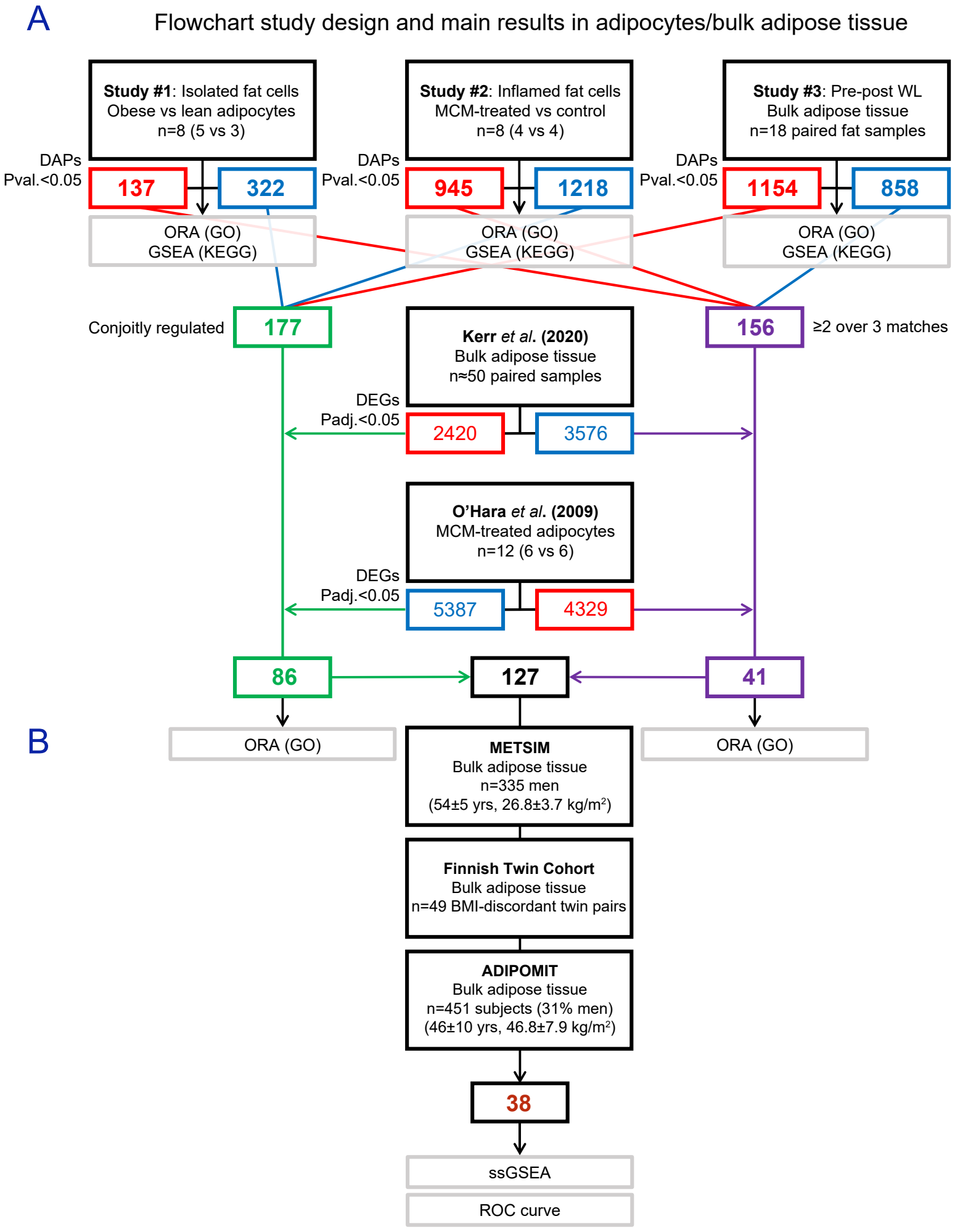
A
Flowchart study design and main results in adipocytes/bulk adipose tissue
Study #1: Isolated fat cells
Obese vs lean adipocytes
n=8 (5 vs 3)
Study #2: Inflamed fat cells
MCM-treated vs control
n=8 (4 vs 4)
Study #3: Pre-post WL
Bulk adipose tissue
n=18 paired fat samples
DAPs
Pval.<0.05
137
322
945
1218
1154
858
ORA (GO)
GSEA (KEGG)
Conjoitly regulated
177
156
≥2 over 3 matches
Kerr et al. (2020)
Bulk adipose tissue
n≈50 paired samples
DEGs
Padj.<0.05
2420
3576
O'Hara et al. (2009)
MCM-treated adipocytes
n=12 (6 vs 6)
5387
4329
86
127
41
B
ORA (GO)
METSIM
Bulk adipose tissue
n=335 men
(54±5 yrs, 26.8±3.7 kg/m²)
Finnish Twin Cohort
Bulk adipose tissue
n=49 BMI-discordant twin pairs
ADIPOMIT
Bulk adipose tissue
n=451 subjects (31% men)
(46±10 yrs, 46.8±7.9 kg/m²)
38
ssGSEA
ROC curve

A

Flowchart study design and main results in EC/adipocytes/bulk adipose tissue

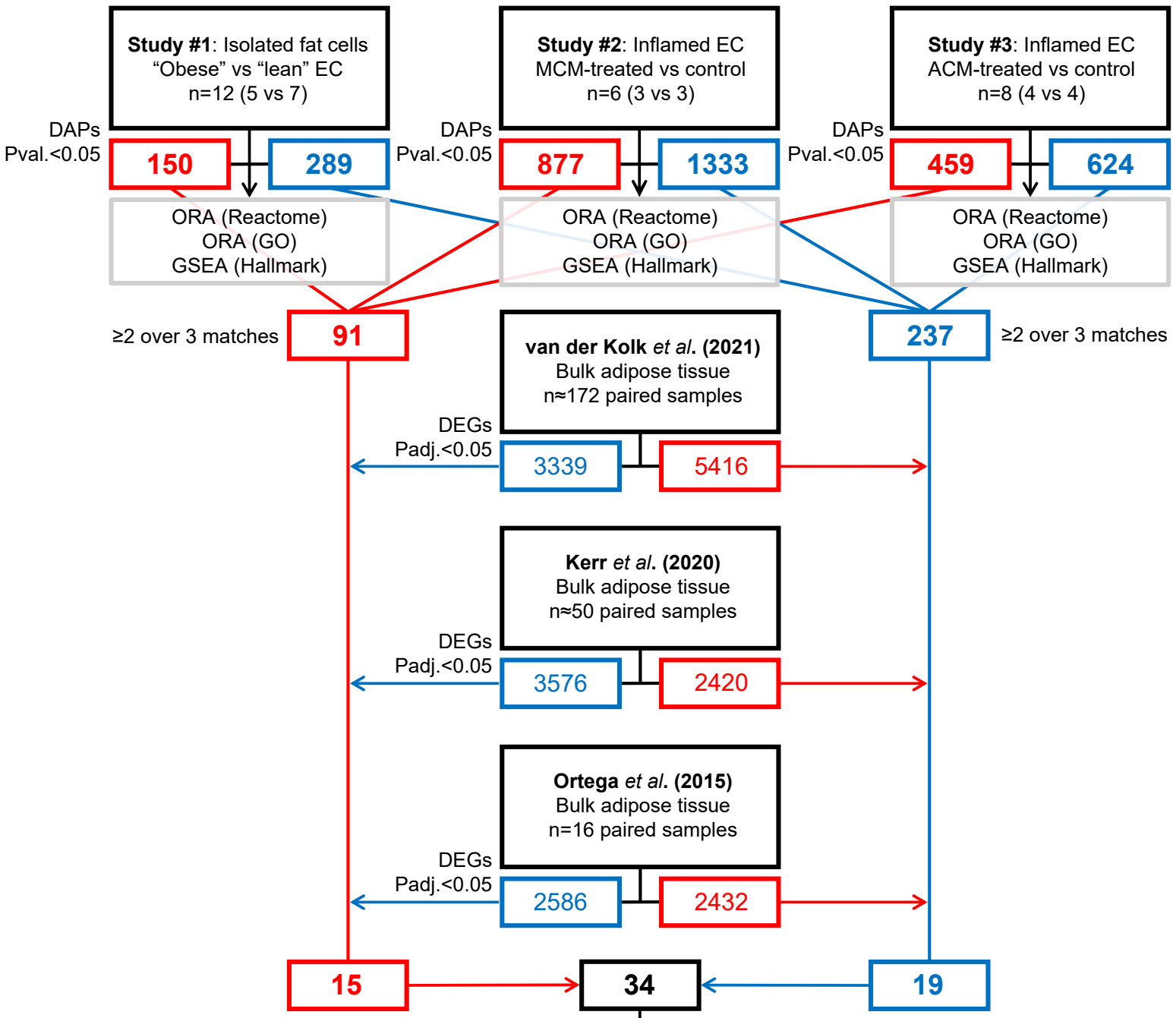

B

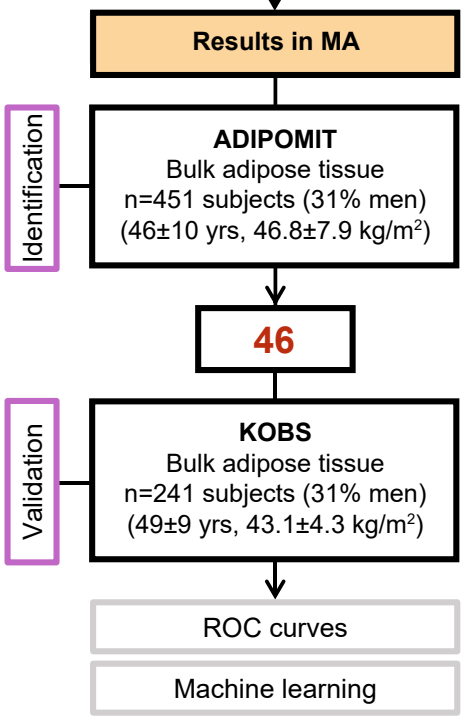

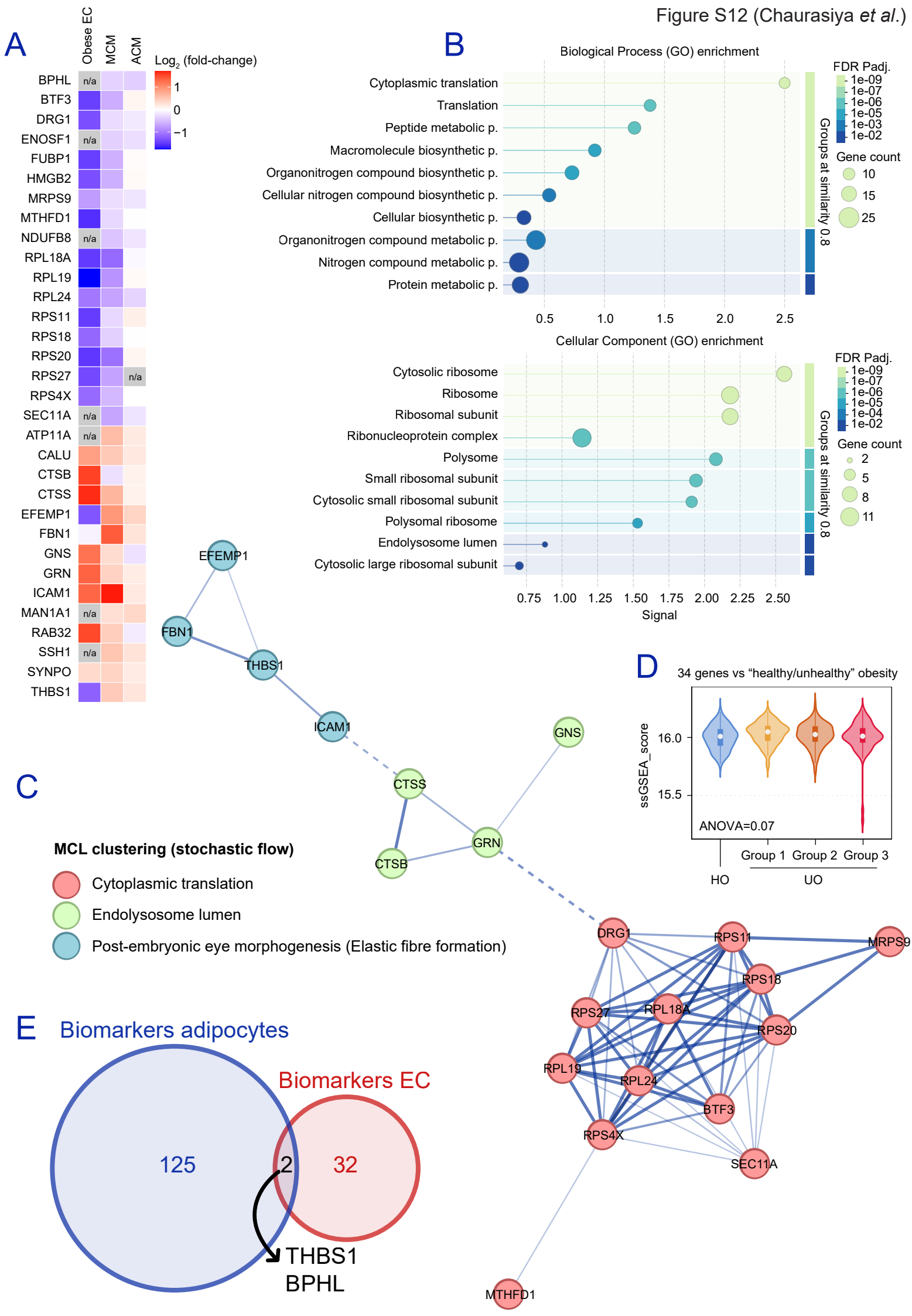
A
Obese EC
MCM
ACM
Log2 (fold-change)
1
0
−1
BPHL
BTF3
DRG1
ENOSF1
FUBP1
HMGB2
MRPS9
MTHFD1
NDUFB8
RPL18A
RPL19
RPL24
RPS11
RPS18
RPS20
RPS27
RPS4X
SEC11A
ATP11A
CALU
CTSB
CTSS
EFEMP1
FBN1
GNS
GRN
ICAM1
MAN1A1
RAB32
SSH1
SYNPO
THBS1
n/a
B
Biological Process (GO) enrichment
Cytoplasmic translation
Translation
Peptide metabolic p.
Macromolecule biosynthetic p.
Organonitrogen compound biosynthetic p.
Cellular nitrogen compound biosynthetic p.
Cellular biosynthetic p.
Organonitrogen compound metabolic p.
Nitrogen compound metabolic p.
Protein metabolic p.
0.5
1.0
1.5
2.0
2.5
FDR Padj.
1e-09
1e-07
1e-06
1e-05
1e-03
1e-02
Gene count
10
15
25
Groups at similarity 0.8
Cellular Component (GO) enrichment
Cytosolic ribosome
Ribosome
Ribosomal subunit
Ribonucleoprotein complex
Polysome
Small ribosomal subunit
Cytosolic small ribosomal subunit
Polysomal ribosome
Endolysosome lumen
Cytosolic large ribosomal subunit
0.75
1.00
1.25
1.50
1.75
2.00
2.25
2.50
Signal
FDR Padj.
1e-09
1e-07
1e-06
1e-05
1e-04
1e-02
Gene count
2
5
8
11
Groups at similarity 0.8
C
MCL clustering (stochastic flow)
Cytoplasmic translation
Endolysosome lumen
Post-embryonic eye morphogenesis (Elastic fibre formation)
EFEMP1
FBN1
THBS1
ICAM1
GNS
CTSS
CTSB
GRN
D
34 genes vs “healthy/unhealthy” obesity
ssGSEA_score
16.0
15.5
ANOVA=0.07
Group 1
Group 2
Group 3
HO
UO
DRG1
RPS11
MRPS9
RPS18
RPS27
RPL18A
RPS20
RPL19
RPL24
BTF3
RPS4X
SEC11A
MTHFD1
E
Biomarkers adipocytes
Biomarkers EC
125
2
32
THBS1
BPHL

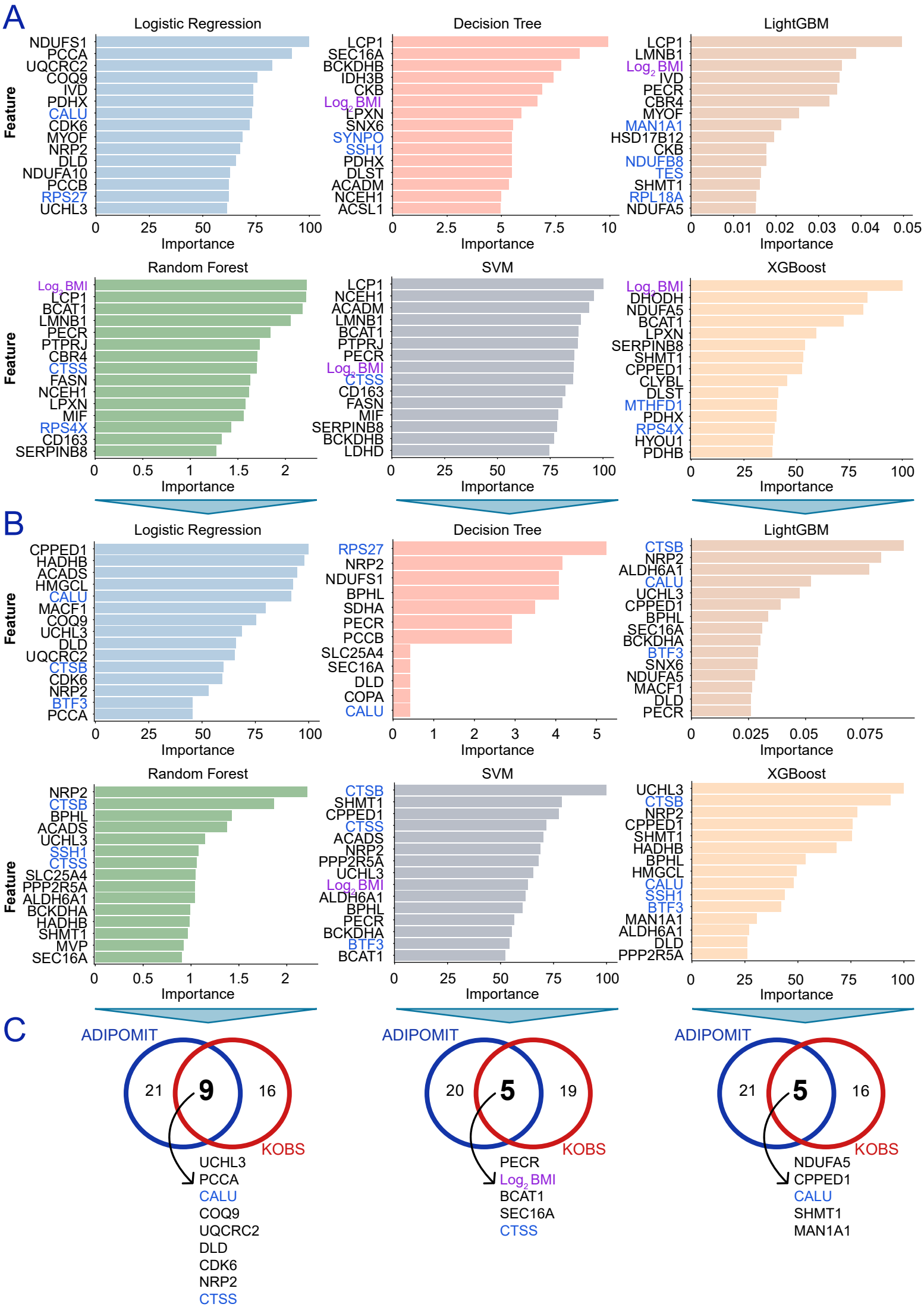
A
Logistic Regression
NDUFS1
PCCA
UQCRC2
COQ9
IVD
PDHX
CALU
CDK6
MYOF
NRP2
DLD
NDUFA10
PCCB
RPS27
UCHL3
Feature
0 25 50 75 100
Importance
Decision Tree
LCP1
SEC16A
BCKDHB
IDH3B
CKB
Log2 BMI
LPXN
SNX6
SYNPO
SSH1
PDHX
DLST
ACADM
NCEH1
ACSL1
0 2.5 5 7.5 10
Importance
LightGBM
LCP1
LMNB1
Log2 BMI
IVD
PECR
CBR4
MYOF
MAN1A1
HSD17B12
CKB
NDUFB8
TES
SHMT1
RPL18A
NDUFA5
0 0.01 0.02 0.03 0.04 0.05
Importance
Random Forest
Log2 BMI
LCP1
BCAT1
LMNB1
PECR
PTPRJ
CBR4
CTSS
FASN
NCEH1
LPXN
MIF
RPS4X
CD163
SERPINB8
Feature
0 0.5 1 1.5 2
Importance
SVM
LCP1
NCEH1
ACADM
LMNB1
BCAT1
PTPRJ
PECR
Log2 BMI
CTSS
CD163
FASN
MIF
SERPINB8
BCKDHB
LDHD
0 25 50 75 100
Importance
XGBoost
Log2 BMI
DHODH
NDUFA5
BCAT1
LPXN
SERPINB8
SHMT1
CPPED1
CLYBL
DLST
MTHFD1
PDHX
RPS4X
HYOU1
PDHB
0 25 50 75 100
Importance
B
Logistic Regression
CPPED1
HADHB
ACADS
HMGCL
CALU
MACF1
COQ9
UCHL3
DLD
UQCRC2
CTSB
CDK6
NRP2
BTF3
PCCA
Feature
0 25 50 75 100
Importance
Decision Tree
RPS27
NRP2
NDUFS1
BPHL
SDHA
PECR
PCCB
SLC25A4
SEC16A
DLD
COPA
CALU
0 1 2 3 4 5
Importance
LightGBM
CTSB
NRP2
ALDH6A1
CALU
UCHL3
CPPED1
BPHL
SEC16A
BCKDHA
BTF3
SNX6
NDUFA5
MACF1
DLD
PECR
0 0.025 0.05 0.075
Importance
Random Forest
NRP2
CTSB
BPHL
ACADS
UCHL3
SSH1
CTSS
SLC25A4
PPP2R5A
ALDH6A1
BCKDHA
HADHB
SHMT1
MVP
SEC16A
Feature
0 0.5 1 1.5 2
Importance
SVM
CTSB
SHMT1
CPPED1
CTSS
ACADS
NRP2
PPP2R5A
UCHL3
Log2 BMI
ALDH6A1
BPHL
PECR
BCKDHA
BTF3
BCAT1
0 25 50 75 100
Importance
XGBoost
UCHL3
CTSB
NRP2
CPPED1
SHMT1
HADHB
BPHL
HMGCL
CALU
SSH1
BTF3
MAN1A1
ALDH6A1
DLD
PPP2R5A
0 25 50 75 100
Importance
C
ADIPOMIT
21
9
16
KOBS
UCHL3
PCCA
CALU
COQ9
UQCRC2
DLD
CDK6
NRP2
CTSS
ADIPOMIT
20
5
19
KOBS
PECR
Log2 BMI
BCAT1
SEC16A
CTSS
ADIPOMIT
21
5
16
KOBS
NDUFA5
CPPED1
CALU
SHMT1
MAN1A1